Neurobiology of Disease 129 (2019) 102–117

Contents lists available at ScienceDirect

Neurobiology of Disease

journal homepage: www.elsevier.com/locate/ynbdi

Voluntary running wheel attenuates motor deterioration and brain damage in cuprizone-induced demyelination

Georgia Mandolesi[a,b,1], Silvia Bullitta[c,1], Diego Fresegna[a], Francesca De Vito[d], Francesca Romana Rizzo[c], Alessandra Musella[a,b], Livia Guadalupi[c], Valentina Vanni[a], Mario Stampanoni Bassi[d], Fabio Buttari[d], Maria Teresa Viscomi[e], Diego Centonze[c,d,*], Antonietta Gentile[c]

[a] Synaptic Immunopathology Lab, IRCCS San Raffaele Pisana, Italy
[b] University San Raffaele, Rome, Italy
[c] Synaptic Immunopathology Lab, Department of Systems Medicine, University of Rome Tor Vergata, Rome, Italy
[d] Unit of Neurology, IRCCS Neuromed, Pozzilli, IS, Italy
[e] Santa Lucia Foundation, IRCCS, Via del Fosso di Fiorano 64, 00143 Rome, Italy

ARTICLE INFO

Keywords:
Demyelination
Multiple sclerosis
Exercise
Cuprizone
Astrogliosis
Microgliosis

ABSTRACT

Growing data from human and animal studies indicate the beneficial effects of exercise on several clinical outcomes in patients with multiple sclerosis (MS), an autoimmune, demyelinating disease, suggesting that it may slow down the disease progression, by reducing brain damage. However, the mechanisms involved are still elusive.

Aim of this study was to address the effects of voluntary running wheel in a toxic-demyelinating model of MS, in which demyelination and brain inflammation occur in response to cuprizone (CPZ) treatment. Mice were housed in standard or wheel-equipped cages starting from the day of CPZ or normal chow feeding for three or six weeks and evaluated for weight changes, locomotor skills and neuromuscular functions over the course of the experimental design. Biochemical, molecular biology and immunohistochemical analyses were performed.

Exercise prevented early weight loss caused by CPZ, indicating improved wellness in these mice. Both neuromuscular function and motor coordination were significantly enhanced by exercise in CPZ-treated mice. Moreover, exercise induced an early protection against axonal damage and the loss of the myelin associated proteins, myelin basic protein (MBP) and 2′,3′-Cyclic-nucleotide 3′-phosphodiesterase (CNPase), in the striatum and the corpus callosum, in coincidence of a strongly attenuated microglia activation in both brain areas. Further, during the late phase of the treatment, exercise in CPZ mice reduced the recruitment of new OLs compared to sedentary CPZ mice, likely due to the precocious protection against myelin damage.

Overall, these results suggest that life-style interventions can be effective against the demyelinating-inflammatory processes occurring in the brains of MS patients.

1. Introduction

Multiple sclerosis (MS) is an autoimmune disorder characterized by recurrent episodes of T cell-mediated immune attacks of the central nervous system (CNS), leading to inflammatory demyelination and secondary axonal damage and progressive disability (Kutzelnigg and Lassmann, 2014). Infiltrating T cells and monocytes/macrophages not only cause oligodendrocyte cell death but also recruit brain resident immune cells, *i.e.* astroglia and microglia, that, in turn, contribute to both the amplification and the resolution of inflammation (Zipp and Aktas, 2006; Popescu and Lucchinetti, 2012). The extent and location of the damage and the failure of reparative mechanisms within the CNS result in a number of symptoms and reduced quality of life (Lublin, 2005). Over the last decades, several disease-modifying therapies (DMTs), have been developed, including immunomodulatory/immunosuppressant agents and, more recently, pro-remyelinating compounds, to slow down disease progression (Barry et al., 2016).

In recent years, there has been considerable interest in possible non-

* Corresponding author at: Department of Systems Medicine, Tor Vergata University, Via Montpellier, 1, 00133 Rome, Italy.
E-mail address: centonze@uniroma2.it (D. Centonze).
[1] Equal contributors

https://doi.org/10.1016/j.nbd.2019.05.010
Received 5 July 2018; Received in revised form 23 October 2018; Accepted 13 May 2019
Available online 14 May 2019
0969-9961/ © 2019 Elsevier Inc. All rights reserved.

pharmacological interventions for MS, such as active-rehabilitation or exercise, to help manage the symptoms of MS and to reinforce the efficacy of DMTs (Motl and Pilutti, 2012; Pilutti et al., 2014). Exercise is well tolerated and induces relevant improvements in both physical and mental functioning in persons with MS (Dalgas et al., 2008), including muscular strength (Dalgas et al., 2009), ambulatory performance (van den Berg et al., 2006), cognition (Ensari et al., 2014) and fatigue (Pilutti et al., 2013; Andreasen et al., 2011), raising the possibility that exercise can halt or slow down pathological processes in MS.

While no perfect mouse model of MS exists, several animal models attempt to examine different aspects of CNS pathology in MS. The cuprizone (CPZ) model provides a reproducible manner to study primary demyelination, inflammation, axonal damage, and myelin repair/remyelination processes (Hiremath et al., 1998; Mason et al., 2000; Schultz et al., 2017), in the absence of peripheral immune system activation (Matsushima and Morell, 2001; Kipp et al., 2009). Indeed, the translational relevance of the CPZ model lies in the fact that the CPZ-induced demyelination closely resembles primary oligodendropathy occurring in lesion type-III and -IV of MS brains (Lucchinetti et al., 2000). CPZ is a copper-chelating mitochondrial agent that selectively targets mature oligodendrocytes of the CNS, especially those of the corpus callosum (CC) (Praet et al., 2014). Demyelination is complete after five weeks of cuprizone intoxication, together with massive microgliosis, astrocytosis and axonal damage (Buschmann et al., 2012). Furthermore, removal of cuprizone from the diet of animals enhances remyelination (Morell et al., 1998).

Aim of this study was to investigate the impact of exercise on motor deficits associated to CPZ model and the underlying pathological hallmarks, namely demyelination, axonal damage and local inflammatory reaction. To address this issue, we used a paradigm of voluntary exercise based on running wheel, which best mimics endurance training in humans (Goh and Ladiges, 2015) and has been convincingly associated with the promotion of wellness in both healthy individuals and subjects affected by neurodegenerative disorders (Cotman and Berchtold, 2002).

2. Materials and methods

2.1. Animals

The subjects of this study were 8-week-old female mice, C57BL/6 N, obtained from Charles-River (Italy). Animals were randomly assigned to standard cages, with two animals per cage, and kept at standard housing conditions with light/dark cycle of 12 h in a temperature-controlled environment (22 °C, 50–60% humidity) and free access to food and water. In order to reduce stress, the animals were manipulated for 1 week before starting the experimental protocol.

Experiments were carried out in accordance with the Internal Institutional Review Committee, the European Directive 2010/63/EU and the European Recommendations 526/2007, and the Italian D.Lgs 26/2014. All efforts were made to minimize the number of animals used.

2.2. Cuprizone (CPZ) model and experimental design

Cuprizone diet and voluntary exercise were started together and mice were sacrificed at the sixt week. Demyelination was induced by feeding mice a diet containing 0.2% cuprizone (CPZ, bis-cyclohexanone oxaldihydrazone; Sigma–Aldrich Inc., St. Louis, MO, USA) mixed into rodent food triturated pellets for 6 weeks (Gudi et al., 2014). At the starting day of the experiment animals were randomly assigned to either voluntary exercise groups fed with standard/0.2% CPZ chow (Control-exercise and CPZ-exercise, respectively) or sedentary groups fed with standard/0.2% CPZ chow (Control and CPZ, respectively) (see also outline in Fig. 1A). CPZ-exercise and Control-exercise groups were housed in cages equipped with a running wheel to allow free access to the wheel. Each wheel was connected to a counter to measure running activity. The sedentary groups were exposed to the same environment, but in cages without wheels.

All animals were sacrificed at the sixt week and tissues for biochemistry, molecular biology and immunohistochemistry were taken.

3. Behavioral analysis

3.1. Body weight

The body weight (g) of each mouse was measured at the end of the first, the third and the fifth week of the experimental period.

3.2. Grip strength test

All mice were tested for grip strength performance using the Grip Strength Meter (Ugo Basile, Italy), as in Gentile et al., 2015, at the end of the first, the third and the fifth week of the experimental period. The Grip Strength Meter consisted of a steel wire grid (8 × 8 cm) connected to an isometric force transducer. Mice were lifted by their tail so that they grasp the grid with their paws. Mice from the four experimental groups were then gently pulled backward until they released the grid and the maximal force in newtons (N) exerted by the mouse before losing the grip was measured. The mean of three consecutive measurements for each animal was calculated.

3.3. Rotarod test

Rotarod analysis is one of the most widely used test to assess motor coordination in rodents. Before performing the test, animals were familiarized with the equipment for one week.

The latency to fall was measured on a rotating rod at an accelerating speed from 4 to 40 rotations/min in 300 s (Harvard Apparatus, UK). After a training phase, the time and the speed at which the mouse fell off the rod were recorded. Each mouse had three trials and the mean latency to fall per trial was calculated. All the mice were evaluated at the Rotarod at the fifth week of demyelination protocol. The test was repeated after a 15-min rest. The length of time the mice stayed on the cylinder correlated with motor coordination and balance; longer times were associated with better coordination and balance (Gentile et al., 2015).

4. Striatal total protein extracts preparation and western blot (WB)

Animals were sacrificed by cervical dislocation at 3 and 6 weeks. Both left and right striata were quickly removed and frozen until use. Tissues were homogenized in RIPA buffer plus protease and phosphatase inhibitors cocktail (SIGMA) as Gentile et al., 2015. After sonication, the homogenates were centrifuged at 13000 ×*g* for 20 min and the supernatant was collected. Protein content was quantified according to the DC Protein Assay method. A quantity of twenty μg of striata extract was denaturated at 95 °C for 5 min and loaded onto a sodium dodecylsulfate polyacrylamide gel [10% for glial fibrillary acidic protein (GFAP) and 2′,3′-Cyclic-nucleotide 3′-phosphodiesterase (CNPase); 15% for myelin basic protein (MBP) and Ionized calcium binding adaptor molecule 1 (IBA1)]. Gels were blotted onto nitrocellulose membrane (Protran; Whatman) and then blocked for 1 h at room temperature (RT) by 5% non-fat dry milk in Tris buffered solution TBS. The following primary antibodies were used: mouse anti-β-actin (1:20000, Sigma) for 1 h RT; rat anti-MBP (1:1000, Millipore) overnight at +4 °C; mouse anti-GFAP (1:4000, Immunological Science) overnight at +4 °C; mouse anti-CNPase (1:1000, Millipore) overnight at +4 °C; rabbit anti-IBA1 (1:500, WAKO). Membranes were incubated with secondary HRP-conjugated IgG anti-mouse (1:10000, 1 h RT for β-actin; 1:4000,1 h RT for GFAP; 1:2000, 1 h RT for CNPase), anti-rat (1:2000,

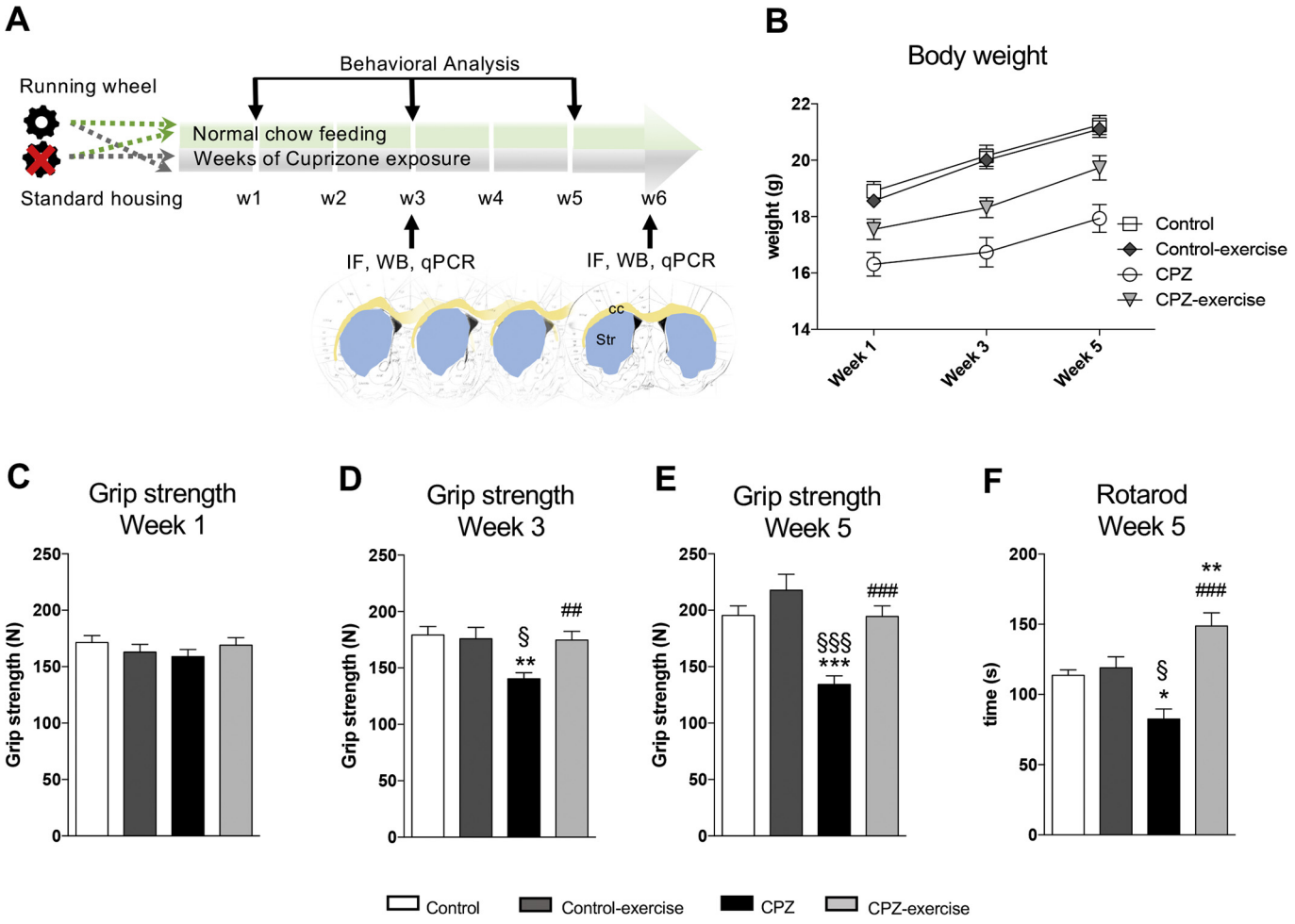

Fig. 1. Voluntary running wheel prevents weight loss, grip strength reduction and impairment of motor coordination in CPZ-treated mice.
A. Outline of the experimental design. The starting day of the experiment mice were divided in 4 groups: mice fed with normal chow and housed in standard cages (Control) or wheel-equipped cages (Control-exercise), mice fed with 0.2% CPZ chow and housed in standard (CPZ) or wheel-equipped cages (CPZ-exercise). All mice were evaluated for behavioral analysis at week 1, 3 and 5. At week 3 and 6 mice were sacrificed for biochemical, molecular biology and histological evaluations in the striatum and the corpus callosum. B. Body weight was assessed over the course of the 5-weeks treatment in Control, Control-exercise, CPZ, CPZ-exercise group. CPZ induced significant weight loss after 1 week of treatment and exercise induced a partial and then a complete recovery in the weight loss induced by CPZ treatment at the third and the fifth week of experimental design, respectively (one-way ANOVA: CPZ *vs* CPZ-exercise $p < 0.05$ week 3, $p < 0.01$ week 5). C. The grip strength test performance was not significantly different among groups during the first week, but it was significantly recovered by physical exercise after three weeks (D) and five weeks (E) of CPZ treatment. (F) Rotarod performance expressed as time (second) to fall off the rod (latency) of CPZ was significantly different in CPZ-exercise mice compared to Control and CPZ-exercise groups. One-way ANOVA, Tukey post-hoc comparisons: $^{\S}p < 0.05$, $^{\S\S\S}p < 0.001$ *vs* Control-exercise; $^{*}p < 0.05$, $^{**}p < 0.01$, $^{***}p < 0.001$ *vs* Control; $^{\#\#}p < 0.01$, $^{\#\#\#}p < 0.001$ *vs* CPZ.

1 h RT for MBP), anti-rabbit (1: 2000, 1 h RT for Iba1). All secondary antibodies were from Amersham GE Healthcare, formerly Amersham Biosciences. After washing, immunodetection was performed by ECL reagent (Amersham GE Healthcare, formerly Amersham Biosciences), and membrane was exposed to film (Amersham GE Healthcare, formerly Amersham Biosciences). Densitometric analysis of protein levels was performed with ImageJ software (http://rsb.info.nih.gov/ij/). WB results were presented as data normalized to control values.

4.1. RNA extraction and qPCR

Murine striata (3 and 6 weeks) were dissected in RNAse-free conditions and total RNA was extracted according to the standard miRNeasy Micro kit protocol (Qiagen). Next, 1400–1800 ng of total RNA were reverse-transcribed using High-Capacity cDNA Reverse Transcription Kit (Applied Biosystems), and 21–45 ng of complementary DNA (cDNA) were amplified in triplicate using the Applied Biosystem 7900HT Fast Real-Time PCR system. SensiMix II Probe Hi-Rox Kit (Bioline; Meridian Life Science) and the following TaqMan gene expression assays were used for the quantification of messenger RNA (mRNAs) coding for interleukin 1 beta (IL1-β), tumor necrosis factor (TNF), transforming growth factor beta 1 (TGF-β1), C-X-C motif chemokine ligand 10 (CXCL10), C-X-C motif chemokine ligand 12 (CXCL12) and beta-actin (ACTB): Il1b mRNA ID: Mm00434228_m1; Tnf mRNA ID: Mm00443258_m1; Tgfb1 mRNA ID: Mm01178820_m1; Cxcl10 mRNA ID: Mm00445235_m1; Cxcl12 mRNA ID: Mm00445553_m1. Relative quantification was performed using the comparative cycle threshold ($2^{-\Delta\Delta Ct}$) method and β-actin was used as endogenous control. All data are expressed relative to control.

4.2. Immunohistochemistry and confocal microscopy

The immunofluorescence (IF) experiments were performed similarly to a method previously described (Gentile et al., 2015). Mice were deeply anesthetized and intracardially perfused with ice-cold 4% paraformaldehyde (PFA) at 3 and 6 weeks (n = 3 Control, n = 3 Control mice, n = 4 CPZ and n = 4 CPZ-exercise for each time-point). Collected brains were post-fixed in 4% PFA for 2 h and equilibrated with 30%

sucrose for at least one night. Thirty-micrometer-thick coronal sections were serially cut on a frozen microtome. One to five sections were taken to analyze the extent of myelination and inflammatory reaction in the whole striatum and the area of the genu of the CC (CCG), from bregma 1.34 to 0.14. Slices were permeabilized in PBS with Triton X-100 0.25% (Tx-PBS). All following incubations were performed in Tx-PBS. To block unspecific sites, sections were pre-incubated with 10% normal donkey serum solution for 2 h RT and then incubated with the primary antibody overnight at +4 °C. Then, after washing, they were incubated with secondary antibodies for 2 h RT and rinsed. Primary antibodies were used as following: rat anti-MBP (1:500); mouse anti-CNPase (1:500); rabbit anti-GFAP (1:500, Dako); rabbit anti-Iba1 (1:500, Wako); mouse anti-SMI32 (1:500; Covance); rabbit anti-Olig2 (1:500; Abcam); mouse anti-APC/CC1 (1:500; Millipore). These were used in combination with the following secondary antibodies: Cy3-conjugated donkey anti-rabbit (1:200; Jackson); Alexa-488-conjugated donkey anti-mouse or anti-rat (1:200; Invitrogen). Nuclei were stained with DAPI. Images were acquired using a LSM7 Zeiss or a Nikon TE2000 confocal laser-scanner microscope with a × 4, ×10, × 20 (zoom × 0.5, 1.5) and × 63 objectives. All images had a pixel resolution of 1024 × 1024. The confocal pinhole was kept at 1.0, the gain and the offset were lowered to prevent saturation in the brightest signals, and sequential scanning for each channel was performed. *Z*-stack images were acquired, z-projected and exported in TIFF file format and adjusted for brightness and contrast as needed, using ImageJ software.

Brain regions were identified using a mouse brain atlas, and central slices containing the CC and the striatum in the bregma interval from 1.34 to 0.14 (Fig. 1) were taken to determine the density of Olig2+ and Olig2 + CC1+ in the lateral areas of the CC. For each animal, four serial sections (one section every five) were processed for immunofluorescence as described above. Z-stacks (10× objective, Z stack interval: 2 µm for a total of twelve slices) were acquired using the same intensity and exposure time. All images were processed using ImageJ software and were adjusted for reducing noise by applying background subtraction as required by the NIH ImageJ. Finally, a projection image derived from 12 images was product. A ROI (region of interest) was designed bilaterally around the region of the CC (see Fig. 5) and the number of Olig2+ or Olig2 + CC1+ cells in the ROI was determined. Data were expressed as cells per mm^2.

A 63× objective (zoom: 1×, z-step: 0.36 µm) was used to detect axons stained with SMI32 antibody. Random field in the CC were chosen from 4 animals per group.

4.3. Statistical analysis

For WB and qPCR experiments, three to five mice per group were employed. For behavioral test at least nine mice per group were analyzed. Throughout the text "n" refer to the number of animals. Data are presented as mean ± SEM. The significance level was established at $p < 0.05$. Differences between two groups were analyzed using two-tailed unpaired Student's *t*-test. Multiple comparisons were analyzed by one-way ANOVA, followed by Tukey's HSD.

5. Results

5.1. Running wheel prevents weight loss and improves motor and neuromuscular function impairment associated to CPZ treatment

Mice exposed to CPZ develop a progressive disease that results in body weight loss and motor dysfunction (Hashimoto et al., 2017). To monitor the effect of exercise on disease progression in the CPZ model, body weight was measured after one, three and five weeks of treatment. In line with previous findings, one week of CPZ treatment induced early weight loss, and exercise induced a partial recovery, even if not statistically significant (Table 1, Fig. 1B; one-way ANOVA analysis Tukey post-hoc: Control *vs* CPZ $p < 0.001$; Control-exercise *vs* CPZ $p < 0.01$). Sedentary CPZ mice weighed significantly less than Control and Control-exercise over the course of five weeks of CPZ intoxication, while CPZ-exercise were significantly different than CPZ at week 3 and 5. In fact, at the third week of treatment the body weight reduction of CPZ mice was partially recovered by exercise (Table 1, Fig. 1B; one-way ANOVA analysis Tukey post-hoc: CPZ *vs* CPZ-exercise $p < 0.05$; Control *vs* CPZ $p < 0.001$; Control *vs* CPZ-exercise $p < 0.05$; Control-exercise *vs* CPZ $p < 0.001$), while after five weeks of treatment, exercise exerted a remarkable effect inducing a complete recovery of body weight (Table 1, Fig. 1B; one-way ANOVA analysis Tukey post-hoc: Control *vs* CPZ $p < 0.001$; Control-exercise *vs* CPZ $p < 0.001$; CPZ *vs* CPZ-exercise $p < 0.05$).

To investigate the effects of exercise on neuromuscular function, we assessed the maximal force of the mice using the grip strength test. At week 1, we did not observe differences in the muscular strength among the experimental groups (Table 1, Fig. 1C; one-way ANOVA analysis, Tukey post-hoc comparisons $p > 0.05$), while at the third week of treatment CPZ induced significant reduction of the strength of both fore- and hind-limbs and exercise showed beneficial effect with a complete recovery of neuromuscular strength (Table 1, Fig. 1D; one-way ANOVA analysis Tukey post-hoc comparisons: Control *vs* CPZ $p < 0.01$; Control-exercise *vs* CPZ $p < 0.05$; CPZ *vs* CPZ-exercise $p < 0.01$). Such beneficial effect of exercise lasted until the fifth week of CPZ treatment (Table 1, Fig. 1E; one-way ANOVA analysis Tukey post-hoc: Control *vs* CPZ $p < 0.001$; Control-exercise *vs* CPZ $p < 0.001$; CPZ *vs* CPZ-exercise $p < 0.001$).

CPZ treatment has been associated with subtle motor dysfunction detectable at Rotarod test (Ye et al., 2013). To address the therapeutic effect of exercise on motor coordination, we performed the Rotarod test at the end of the exercise protocol. Rotarod analyses demonstrated that mice of the CPZ group had shorter latency to fall compared with both Control and Control-exercise groups, and, CPZ-exercise animals performed significantly better than CPZ and Control mice (Table 1, Fig. 1F; one-way ANOVA analysis Tukey post-hoc: Control *vs* CPZ $p < 0.05$; Control *vs* CPZ-exercise $p < 0.01$; Control-exercise *vs* CPZ $p < 0.05$; CPZ *vs* CPZ-exercise $p < 0.001$), suggesting that voluntary exercise was effective against typical motor deficits induced by CPZ.

5.2. Voluntary running wheel reduces CPZ-induced demyelination

CPZ induces a highly reproducible demyelination in distinct brain regions, among which the CC represents the most frequently investigated white matter tract (Stidworthy et al., 2003). The striatum, an important area of the basal ganglia involved in motor activity (Grace, 2002), undergoes demyelination during CPZ treatment (Pott et al., 2009), as well.

We investigated whether physical exercise may have an impact on demyelination extent in this model. We measured the striatal protein levels of the myelin basic protein (MBP), marker for myelin, after 3 and 6 weeks of CPZ treatment. MBP was shown down-regulated already after three weeks of CPZ feeding in both the CC and the striatum (Pott et al., 2009; Hiremath et al., 1998; Stidworthy et al., 2003). In our experimental settings we found that the loss of MBP protein induced by 3 weeks of CPZ feeding was almost recovered by exercise. Indeed, CPZ-exercise experimental group was not significantly different compared to both control and CPZ groups (Fig. 2A-A′; MBP/β-actin ratio: Control: 1 ± 0.02, n = 3; CPZ: 0.53 ± 0.06, n = 5; CPZ-exercise: 0.79 ± 0.13, n = 4; one-way ANOVA analysis Tukey post-hoc: Control *vs* CPZ $p < 0.05$; Control *vs* CPZ-exercise $p > 0.05$; CPZ *vs* CPZ-exercise $p > 0.05$). Interestingly, the analysis of striatal samples taken at the end of the treatment (6 weeks) showed that exercise significantly attenuated the CPZ-induced loss of MBP (Fig. 2B-B′; MBP/β-actin ratio: Control: 1 ± 0.14, n = 8; CPZ: 0.14 ± 0.02, n = 10; CPZ-exercise: 0.44 ± 0.07, n = 10; one-way ANOVA analysis Tukey post-hoc: Control *vs* CPZ $p < 0.001$; Control *vs* CPZ-exercise $p < 0.001$; CPZ *vs* CPZ-exercise $p < 0.05$). Physical exercise has been reported to affect

Table 1
Behavioral data of mice at week 1, 3 and 5 of the experimental design.

Test	Week	Control n = 15	Control-exercise n = 9	CPZ n = 18	CPZ-exercise n = 16
Weight (g)	1	18.9 ± 0.340	18.56 ± 0.223	16.31 ± 0.417§§ ***	17.55 ± 0.361
	3	20.16 ± 0.374	20 ± 0.303	16.74 ± 0.518§§***	18.31 ± 0.357$^{§\#}$
	5	21.25 ± 0.346	21.10 ± 0.294	17.94 ± 0.496***§§§	19.73 ± 0.438$^{\#}$
Grip strength (N)	1	171.5 ± 0.095	162.9 ± 6.868	158.9 ± 6.285	169 ± 6.741
	3	179.3 ± 7.524	175.9 ± 10.08	140.5 ± 5.374§**	174.7 ± 7.721$^{\#\#}$
	5	195.5 ± 8.451	217.7 ± 14.13	134.2 ± 7.606§§§***	194.6 ± 9.274$^{\#\#\#}$
Rotarod (s)	5	113.6 ± 3.892	119.1 ± 7.827	82.52 ± 7.091§*	148.7 ± 9.533$^{*\#\#\#}$

Data are expressed as mean ± sem. Comparison of CPZ and CPZ-exercise to Control * $p < 0.05$, ** $p < .0.01$, *** $p < 0.001$; comparison of CPZ and CPZ-exercise to Control-exercise $^{§§}p < 0.05$, $^{§§}p < 0.01$, $^{§§§}p < 0.001$; comparison between CPZ and CPZ-exercise $^{\#}p < 0.05$, $^{\#\#}p < 0.01$, $^{\#\#\#}p < 0.001$. One-way ANOVA analysis Tukey post-hoc.

myelination, with various effects according to the analyzed brain area (Yoon et al., 2016; Tomlinson et al., 2018). For this reason, we assessed whether physical exercise may induce changes in myelin content *per se*, analyzing the protein level of MBP in Control-exercise mice compared with Control mice. In our experimental conditions and in accordance with Tomlinson et al. (2018), there were no statistically significant differences in MBP protein levels between the two experimental groups after six weeks of treatment (Fig. 2C-C′; MBP/β-actin ratio: Control: 1 ± 0.10, n = 5; Control-exercise: 0.96 ± 0.10, n = 5; Unpaired *t*-test $p > 0.05$).

Next, we performed immunohistochemistry on corticostriatal slices taken from Control, CPZ and CPZ-exercise mice to support the biochemical studies, and to address the myelination extent in both the CC and the striatum at week 3 and 6 of the experimental setting. During the treatment, the CPZ-induced demyelination showed a gradual development starting from the lateral areas of both the striatum and the CC to the medial area of the CC. As shown in Fig. 2D, after 3 weeks of CPZ feeding myelin loss was evident in the lateral callosal projection and in the striosomes, the packed myelinated axons, located in the lateral striatum (Fig. 2D, upper panel, red arrows). At week 6, CPZ induced an even more significant loss of MBP in the external callosal projection and external capsule (EC) up to extend to the surrounding white matter area of the cingulum (CG) (Fig. 2D, low magnification image, middle panel). At this time-point the striosomes placed in lateral parts of the striatum were completely demyelinated, while those in the area close to the lateral ventricle (LV) were less affected, in accordance with previous data (Pott et al., 2009) (Fig. 2D, red arrows in middle and bottom panel).

Exercise ameliorated myelin pathology observed in CPZ brains throughout the period of CPZ feeding. Indeed, running wheel exposure preserved myelin density in the areas affected by CPZ at week 3 (lateral callosal projection and striosomes-Fig. 2D, upper panel). Such effect was remarkably more evident after six weeks of treatment. As shown in the low magnification images (Fig. 2D, middle panel), exercise increased the staining for MBP in demyelinated areas of CC, CG and striatum, without inducing gross recovery of MBP labelling in the lateral striatum. At higher magnification it was possible to better appreciate differences in MBP-labelled myelin fibers in both the CC and the striatum among the three experimental groups. In control slices myelin fibers were dense and deeply-stained in the CC and the striatum, while in myelin fibers of the same brain structures of CPZ mice holes indicative of lack of MBP staining were frequently visible (red arrows). The pattern of myelin staining was rather preserved in CC and striosomes of CPZ-exercise animals.

The 2′,3′-Cyclic-nucleotide 3′-phosphodiesterase (CNPase) is a myelin protein exclusively expressed by mature oligodendrocyte in the CNS and considered a marker for myelin forming cells (Bercury and Macklin, 2015). Moreover, CNPase has been shown to be implicated in MS pathogenesis, playing a role as an autoantigen (Muraro et al., 2002). To further confirm the efficacy of physical exercise against an ongoing demyelination process, we examined CNPase protein levels in the striatum of Control, CPZ and CPZ-exercise mice. CNPase was already downregulated after 3 weeks of CPZ feeding and, as observed for MBP, exercise exerted a beneficial effect with a trend in the recovery of the protein levels in the analyzed striatal samples (Fig. 3A-A'; CNPase/β-actin ratio: Control: 1 ± 0.09, n = 4; CPZ: 0.50 ± 0.11, n = 5; CPZ-exercise: 0.89 ± 0.12, n = 4; one-way ANOVA analysis Tukey post-hoc: Control *vs* CPZ $p < 0.05$; Control *vs* CPZ-exercise $p > 0.05$; CPZ *vs* CPZ-exercise $p > 0.05$). At week 6, a further significant drop of CNPase levels in CPZ striatum was observed and voluntary exercise partially prevented such loss (Fig. 3B-B′; CNPase/β-actin ratio: Control: 1 ± 0.08, n = 8; CPZ: 0.09 ± 0.045, n = 7; CPZ-exercise: 0.31 ± 0.035, n = 10; one-way ANOVA analysis Tukey post-hoc: Control *vs* CPZ $p < 0.001$; Control *vs* CPZ-exercise $p < 0.001$; CPZ *vs* CPZ-exercise $p < 0.05$). We assessed whether physical exercise could alter *per se* CNPase content in striatal lysates, by analyzing the CNPase levels in Control-exercise and Control mice. In agreement with previous data (Yoon et al., 2016), no statistically significant differences in protein levels of CNPase between the two experimental groups could be detected (Fig. 3C-C'; CNPase/β-actin ratio: Control: 1 ± 0.04, n = 5; Control-exercise: 0.90 ± 0.07, n = 5; Unpaired *t*-test $p > 0.05$).

We also evaluated the pattern of expression of CNPase in the CC and the striatum by IF. In CPZ brains CNPase staining in both areas closely resembled that observed for MBP in the CC and the striatum at both time-points (3 and 6 weeks) (Fig. 3D). Indeed, significant loss of CNPase was observed at the level of CC and striatum in CPZ brains and a partial recovery was found in CPZ-exercise brains already at week 3 (Fig. 3D, upper panel). At week 6 CNPase staining revealed an extent of demyelination in CPZ and CPZ-exercise similar to that detected with MBP (see yellow arrows in the low magnification image in Fig. 3D, middle panel). In Fig. 3D areas of CNPase loss and recovery are highlighted by yellow arrows in CPZ and CPZ-exercise slices, respectively (Fig. 3D, bottom panel).

5.3. Preventive beneficial effect of exercise on the late recruitment of new oligodendrocytes (OLs)

Regional differences in the dynamics of OLs differentiation and remyelination in response to CPZ have been described (Baxi et al., 2017). In the midline CC, the number of mature OLs after a consistent reduction around 3–4 weeks of CPZ feeding, raises to normal density at week 6, in coincidence of the spontaneous remyelination, occurring between week 5 and 6 (Baxi et al., 2017). Notably, such OLs repopulation of the CC is not followed by a histochemical detection of myelin extent recovery, implying an incomplete remyelination which is faster and detectable after CPZ withdrawal from the diet. To account for the myelin preservation observed at 3 and 6 weeks, we assessed the effect of exercise on OLs loss (3 weeks) and recruitment (6 weeks). We determined the density of cells expressing the transcription factor Olig2, expressed in both oligodendrocyte precursor cells (OPCs) and OLs, and the adenomatous polyposis coli CC1 (APC)-CC1, a marker of mature OLs, in the lateral CC that, based on our previous results, was particularly

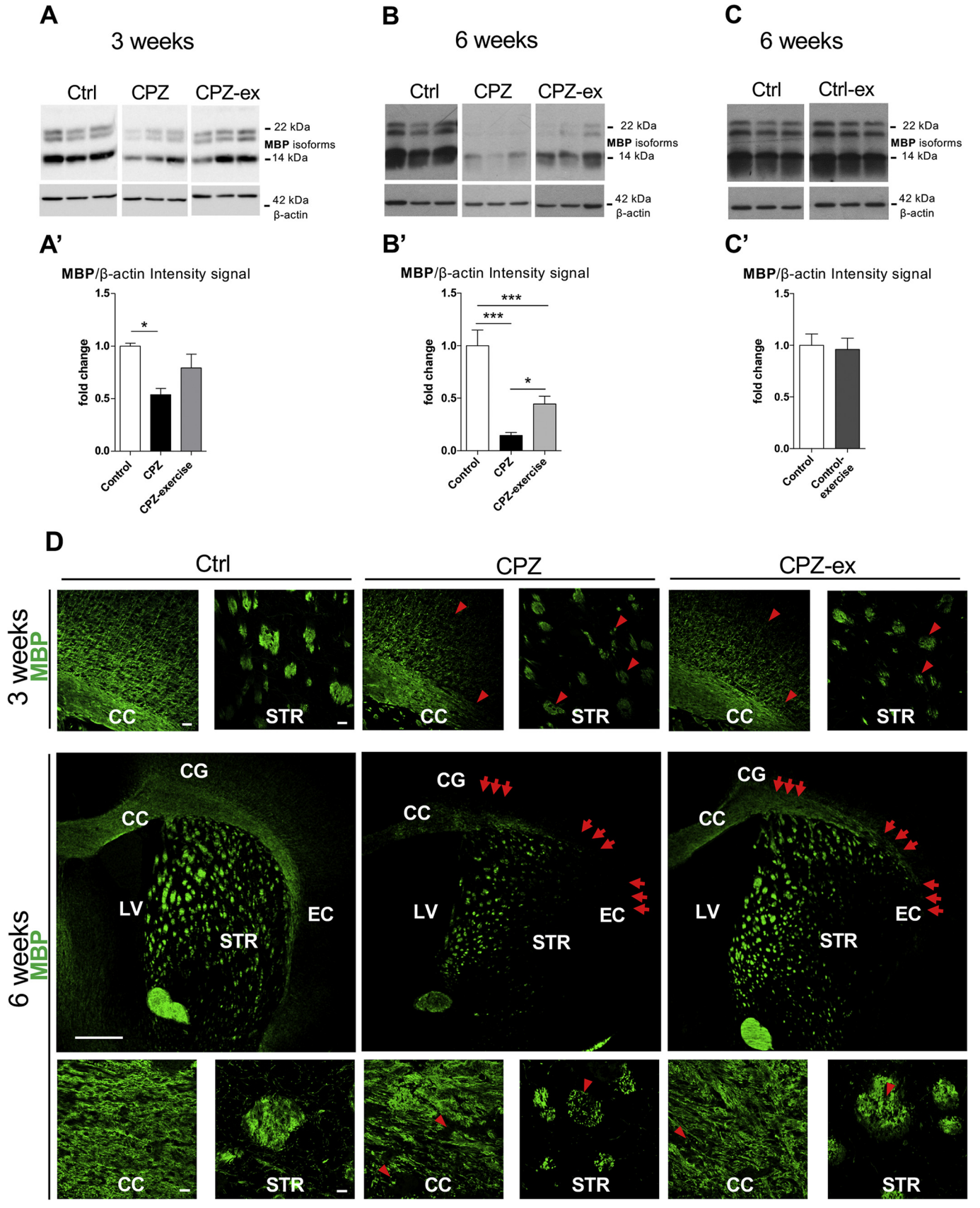

(caption on next page)

Fig. 2. Voluntary running wheel lessens demyelination in both the corpus callosum and the striatum of CPZ-treated mice.
A-A'. In the third week, a biochemical study of MBP protein was carried out on striatal protein extracts from control, CPZ and CPZ-exercise mice. Western blot densitometric analysis shows that the MBP protein level was significantly low in striatal lysates of CPZ compared to control samples and, although not statistically significant, exercise induced a recovery of MBP levels at this time-point. One-way ANOVA, Post-hoc Tukey comparisons: * $p < 0.05$. The panel in B-B′ shows that, after six weeks of treatment, the MBP protein level related to β-actin was significantly increased in striatal lysates of CPZ exercise compared to CPZ samples. One-way ANOVA; Tukey post-hoc comparisons: * $p < 0.05$; *** $p < 0.001$. C-C′. No statistically significant differences in protein levels of MBP between Control and Control-exercise were observed in WB experiments. Unpaired *t*-test $p > 0.05$. D. Coronal sections of Control, CPZ and CPZ-exercise brains were stained with MBP antibody (green fluorescence). Confocal microscopy images highlight early demyelination after 3 weeks of CPZ feeding, particularly in the lateral callosal projection and the striosomes placed in lateral parts of the striatum. Running wheel exposure preserved myelin density in the areas affected by CPZ at week 3 (upper panel, scale bar: 50 μm). At week 6, in CPZ-exercise slices MBP staining is preserved in almost the analyzed area with less remarkable effects in the external part of the striatum that is heavily affected by CPZ treatment. Low magnification images show the extent of demyelination induced by CPZ in the corpus callosum (CC), including the external capsula (EC), the cingulum (CG), and peripheral area of the striatum and a less intense staining in the lateral part close to the lateral ventricle (LV), (middle panel, scale bar: 600 μm). Lower panel (high magnification images, scale bar: 10 μm) highlights differences in myelination in the CC and striosomes of Control, CPZ and CPZ-exercise brains. Compared to Control slices, CPZ reduced the density of MBP-labelled myelin fibers (red arrows indicate lack of MBP staining), while exercise partially recovered MBP staining. Red arrows in the pictures indicate areas of gross morphological changes and loss of MBP staining. (For interpretation of the references to color in this figure legend, the reader is referred to the web version of this article.)

vulnerable to CPZ treatment and partially preserved by exercise. At week 3 the density of Olig2+ cells was reduced in the CC of CPZ mice (Fig. 4A-A") and, in both Control and CPZ mice, exercise induced a similar reduction of Olig2+ cells, although the One-way ANOVA statistical test revealed significant differences only between CPZ-exercise and Control mice (Fig. 4A-A'"; cell density: Control 0.52 ± 0.02 n = 3, Control-exercise 0.39 ± 0.02 n = 3, CPZ 0.32 ± 0.06 n = 4, CPZ-exercise 0.28 ± 0.053 n = 4; one-way ANOVA analysis Tukey post-hoc: $p < 0.05$ CPZ-exercise *vs* Control). By comparing the number of Olig2 + CC1+ cells among the four experimental groups we observed that the density of this population was significantly reduced in both CPZ and CPZ-exercise (Fig. 4A-A'"; cell density: Control 0.19 ± 0.01, Control-exercise 0.14 ± 0.02, CPZ 0.06 ± 0.01, CPZ-exercise 0.07 ± 0.02; one-way ANOVA analysis Tukey post-hoc: $p < 0.01$ CPZ *vs* Control, $p < 0.05$ CPZ-exercise *vs* Control). Surprisingly, the analysis of cell density in Control-exercise mice highlighted a drop of Olig2 + CC1+ cells in the presence of normal myelin. Based on the observation that exercise could have an effect *per se* on this cell population, we suggest that in mice fed with CPZ, exercise did not induce a further drop in Olig2 + CC1+ cells, highlighting a reduced loss of Olig2 + CC1+ density in CPZ-exercise group compared to CPZ. This might explain the finding that in CPZ-exercise the myelin pattern was more similar to Control and Control-exercise (Fig. 4A', double staining CC1, red color, and MBP, green color).

At week 6 we found an increase of Olig2+ cells in CPZ CC that, by one-way ANOVA, was significantly different only from Control-exercise group (Fig. 4B-B"; cell density: Control 0.51 ± 0.03, Control-exercise 0.27 ± 0.14, CPZ 0.71 ± 0.05, CPZ-exercise 0.51 ± 0.09; one-way ANOVA analysis Tukey post-hoc: $p < 0.05$ CPZ *vs* Control-exercise). The measure of Olig2 + CC1+ density in CPZ mice highlighted a significant increase relative to both control groups (Fig. 4B-B'": cell density: Control 0.15 ± 0.01, Control-exercise 0.08 ± 0.03, CPZ 0.34 ± 0.01, CPZ-exercise 0.21 ± 0.03; one-way ANOVA analysis Tukey post-hoc: $p < 0.01$ CPZ *vs* Control, $p < 0.001$ CPZ *vs* Control-exercise). These data likely reflect the spontaneous OLs repopulation in the CC occurring at 6 weeks of CPZ, which, however, is unsuccessful by virtue of the lack of myelin recovery, as highlighted in Fig. 4B' (double staining CC1, red color, and MBP, green color) and Figs. 2 and 3. Interestingly, the recruitment of new OLs in the CPZ-injured region was milder in CPZ-exercise mice ($p < 0.05$ CPZ-exercise *vs* Control-exercise; $p < 0.05$ CPZ *vs* CPZ-exercise), as expected in this experimental group characterized by the precocious reduced demyelination (Fig. 4B', double staining CC1, red color, and MBP, green color).

Furthermore, at 6 weeks we observed a gradient of distribution of the recruited Olig2 + CC1+ in the CC with a higher concentration of the cells in the external part of the CC compared to that close to the LV and the midline CC (Fig. B). In that zone (yellow Roi in the picture) the number of Olig2 + CC1+ cells in CPZ CC was similar to Control, confirming previous study (Baxi et al., 2017) and suggesting that at 6 weeks of CPZ feeding in the lateral callosal projection the recruitment of new OLs is remarkably accelerated compared to other regions of the CC (Fig. 4B-B'": cell density Control 0.13 ± 0.01, Control-exercise 0.06 ± 0.03, CPZ 0.135 ± 0.02, CPZ-exercise 0.09 ± 0.01; one- way ANOVA $p > 0.05$). Importantly, the recruitment of new OLs was lower in CPZ-exercise compared to CPZ even in this area.

5.4. Running wheel protects against axonal damage in CPZ CC

Together with demyelination, another typical hallmark of MS brain is axonal damage, characterized by several morphological changes, including transection, swelling, rearrangements of neurofilaments and alterations of axonal caliber (Trapp et al., 1998). Similar axonal pathology occurs in the brain of CPZ mice, as well (Gudi et al., 2017).

To study the effects of exercise on axonal pathology of the injured CPZ brain, we performed IF experiments, using an antibody that selectively labels unphosphorylated neurofilaments, aka SMI32, and that is a validated marker of neuro-axonal damage (Gudi et al., 2017). Neurofilaments are the main components of neuronal cytoskeleton involved in axonal transport. In healthy axons they are mostly phosphorylated, while the dephosphorylated forms of neurofilaments reside in dendrites and neuronal soma. Therefore, accumulation of dephosphorylated neurofilaments in axons has been linked to pathological conditions of neuronal degeneration with impaired axonal conduction (Yuan et al., 2017).

We focused on the lateral callosal projections, where at high magnification SMI32 staining was circumscribed to few myelinated axons in Control slices (Fig. 5A, double IF for SMI32-red color, MBP-green color). After 3 weeks of CPZ treatment we could observe an intense staining for SMI32 and, importantly, in areas of overt demyelination, as highlighted by the lack of MBP signal. Moreover, axonal interruptions, typical of pathological axon conduction, could be detected in that area (yellow arrows) (Fig. 5B). At the same time-point in CPZ-exercise brains we observed a less intense SMI32 in the presence of a more intense MBP staining (Fig. 5C, yellow arrows). A week 6, SMI32 staining revealed an increased staining of the axons for SMI32 in both CPZ and CPZ-exercise compared to control (in A), with more intense MBP labelling in CPZ slices. However, SMI32 staining was remarkably higher in CPZ than in CPZ-exercise, highlighting severe axonal accumulation of dephosphorylated neurofilaments (Fig. 5D-E, yellow arrows in the picture). These data suggest that exercise induced an early protection of axons during the course of CPZ feeding.

5.5. Astrogliosis is attenuated in CPZ-exercise mice

A typical hallmark of both MS lesions and CPZ-induced demyelination is the accumulation of reactive astrocytes and microglia within the damaged CNS areas (Clarner et al., 2012). Astrogliosis and microgliosis have been claimed to play a dual role in myelin disorders,

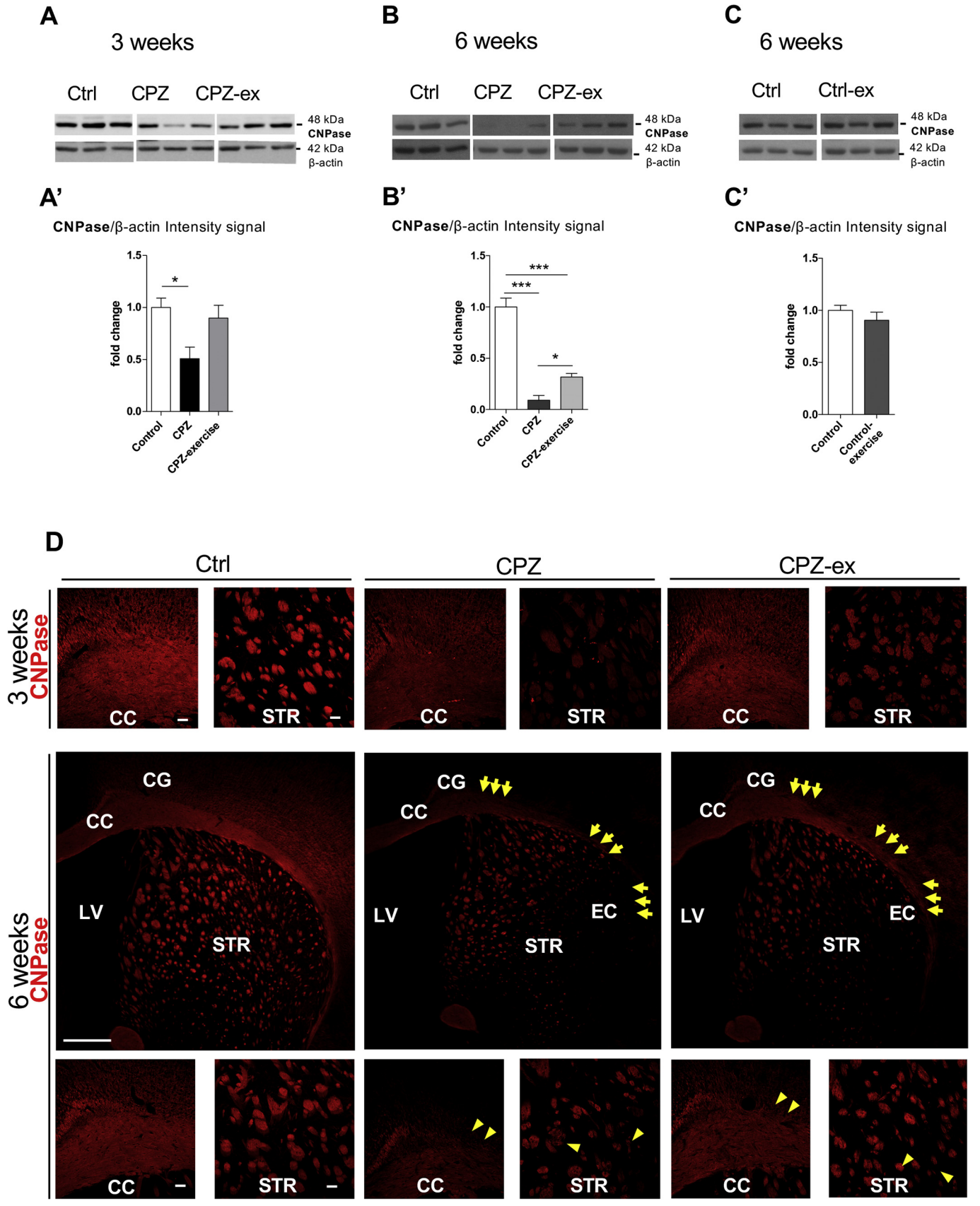

(caption on next page)

Fig. 3. Voluntary running wheel attenuates CNPase down-regulation in both the striatum and the corpus callosum of CPZ-treated mice.
A-A'. Representative blot showing CNPase and β-actin bands of Control, CPZ and CPZ-exercise striatal lysates, taken after 3 weeks of treatment. Band densitometry shows that 3-weeks voluntary exercise induced a strong trend in the recovery of the protein levels in the CPZ striatum. One-way ANOVA, Tukey post-hoc comparisons: * $p < 0.05$. B, B′. Blot image and densitometric analysis show that six weeks of voluntary exercise significantly attenuated the loss of protein expression of CNPase induced by CPZ. One-way ANOVA, Tukey post-hoc comparison: * $p < 0.05$; *** $p < 0.001$. C-C′. No statistically significant differences in protein levels of CNPase between Control and Control-exercise groups were detected. Unpaired *t*-test $p > 0.05$. D. CNPase antibody was used to stain oligodendrocytes at the level of CC, CG and striatum. At week 3, CNPase staining (red fluorescence) is less intense in both the CC and the striatum of CPZ mice compared to both Control and CPZ-exercise slices (upper panel, scale bar: 50 μm). High magnification images of brains taken at 6 weeks show the extent of CNPase staining, which closely resembles that of MBP in all the experimental groups (middle panel, scale bar: 400 μm). The recovery in CNPase staining is highlighted in high magnification images in the bottom panel (scale bar: 50 μm). Yellow arrows in the pictures indicate areas of gross morphological changes and loss of CNPase staining. (For interpretation of the references to color in this figure legend, the reader is referred to the web version of this article.)

meaning that they can participate in both the resolution and the promotion of inflammatory reactions, resulting in myelin repair and damage, respectively (Domingues et al., 2016).

We analyzed the effects of exercise on CPZ-induced astrogliosis. At week 3 extensive astrogliosis, detected with an antibody against the astrocyte marker GFAP, was observed in the CC and the striatum of CPZ mice and the effects of exercise seemed to be moderate and variable in both areas (Fig. 6A). WB data for GFAP confirmed this observation (Fig. 6B-B'; GFAP/β-actin ratio Control: 1 ± 0.15, n = 4; CPZ: 10.24 ± 2.0, n = 5; CPZ-exercise: 8.33 ± 2.15, n = 5; one-way ANOVA analysis Tukey post-hoc: Control *vs* CPZ $p < 0.05$; Control *vs* CPZ-exercise $p < 0.05$; CPZ *vs* CPZ-exercise $p > 0.05$). At week 6 IF experiments showed that astrogliosis was still strongly high in CPZ brains, in line with previous findings (Skripuletz et al., 2013), and partially reduced in CPZ-exercise brains (Fig. 6C, red staining for GFAP). WB experiments supported the histochemical evaluation, revealing the significant effect of exercise in dampening astroglia reaction, although the degree of reduction was about 5% (Fig. 6D-D'; GFAP/β-actin ratio Control: 1 ± 0.65, n = 8; CPZ: 29.89 ± 1.28, n = 10; CPZ-exercise: 24.56 ± 1.62, n = 10; one-way ANOVA analysis Tukey post-hoc: Control *vs* CPZ $p < 0.001$; Control *vs* CPZ-exercise $p < 0.001$; CPZ *vs* CPZ-exercise $p < 0.05$).

Both astroglia and microglia contribute to foster the local inflammatory reaction in MS lesions and CPZ brains, by releasing soluble mediators. By qPCR we analyzed the expression of cytokines (TNF, IL-1β) and chemokines (TGF-β, CXCL12 and CXCL10) in striatal samples taken at week 3 and 6 of the experimental design. As expected, the mRNAs of the above molecules were significantly increased in the CPZ group compared to both Control and Control-exercise group during the whole CPZ challenge span, except for CXCL12 (Table 2). Among the inflammatory mediators analyzed, only CXCL10 was significantly reduced by exercise at week 6 (Table 2).

5.6. Exercise significantly lessens microgliosis in CPZ brains

Next, we analyzed the effect of exercise on microglia activation during the time-course of CPZ treatment. Brain slices were stained with an antibody raised against Iba1, marker of microglia/macrophage. As expected, an extensive staining for Iba1 was evident in CPZ brain slices, and exercise elicited a strong inhibitory effect, as highlighted in the IF images in Fig. 7A (red color Iba1). The life cycle of microglia includes the shift from a resting phenotype under normal circumstances to activated or reactive states (Lynch, 2009). At this time-point, in both experimental groups cells intensely stained for Iba1 and with a morphology resembling amoeboid/phagocytic microglia (activated microglia) were found in the whole CC, although they were less frequently observed in CPZ-exercise brains (round shaped Iba1+ cells highlighted by yellow arrows and inset on the right in Fig. 7A), while less-intensely stained cells were more frequent in CPZ-exercise (yellow arrows and inset on the right in Fig. 7A). Of note, at this time-point in the lateral callosal projections of CPZ brains, already depicted in Fig. 4A', extensive microgliosis was associated with areas of myelin loss (Fig. 7A', yellow arrows in MBP staining). In the same area of CPZ-exercise slices a reduced microglia activation was observed in association with less damaged myelin (Fig. 7A').

At week 6 the IF analysis of Iba1 (red staining in the picture) showed a reduced microgliosis in CPZ compared to 3-week CPZ in line with previous data showing a reduction of microglia at 6 weeks of CPZ feeding (Skripuletz et al., 2013). Even at this time-point exercise significantly attenuated microgliosis (low magnification image in upper panel in Fig. 7B). Moreover, while resting microglia (with elongated and ramified processes) was clearly visible in Control slices (bottom panel in Fig. 7B), microglia phenotype in CPZ more likely resembled those of intermediate states of activated microglia, with an increase in cell body and thickness of elongations, both intensely stained. CPZ-exercise microglia showed a less intense staining compared to CPZ, likely indicating a different or alternative activated state (Lynch, 2009). Moreover, WB experiments performed on striatal lysates taken at 6 weeks supported the IF analysis, showing that Iba1 levels were reduced by half in CPZ-exercise striata (Fig. 7C-C′; Iba1/β-actin ratio: Control: 1 ± 0.09, n = 4; CPZ: 6.04 ± 1.03, n = 4; CPZ-exercise: 3.12 ± 0.49, n = 5; one-way ANOVA analysis Tukey post-hoc: Control *vs* CPZ $p < 0.001$; Control *vs* CPZ-exercise $p > 0.05$; CPZ *vs* CPZ-exercise $p < 0.05$).

6. Discussion

In the present investigation we provided first evidence for the beneficial effects of voluntary exercise during toxic central demyelination. Voluntary running wheel was able to prevent motor activity deficits and weight loss induced by CPZ feeding, suggesting improved well-being. Functional recovery promoted by exercise was linked to limited myelin destruction and loss of myelin-associated proteins in white matter tracts of the CC, the CG and the striatum and reduced axonal pathology. Moreover, exercise significantly attenuated innate immune response, namely microgliosis and, to a lesser extent, astrogliosis.

In rodents, behavioral experiences, including exercise, have been convincingly associated with significant brain anatomical changes in terms of weight and size, hippocampal neurogenesis and synaptogenesis (van Praag et al., 2000), and synaptic plasticity (Patten et al., 2013). The effects of exercise may depend on the experimental paradigms used. Indeed, while forced exercise, like treadmill training, may induce stress that, in turn, may act as a confounding factor, voluntary running wheel is considered devoid of the stressful components and represents a good tool to investigate brain activity changes under physiological and pathological conditions. Notably, voluntary exercise has been shown to attenuate clinical and pathological hallmarks in animal models of neurological disorders, including Parkinson's Disease (PD) (Klein et al., 2016), Hungtinton's Disease (HD) (Herbst and Holloway, 2015), Alzheimer's Disease (AD) (Tapia-Rojas et al., 2016) and Rett Syndrome (Kondo et al., 2016). In the context of MS, several paradigms of forced and voluntary exercise have been used to address the effects of physical training on disease course in the MS mouse model, EAE. In particular, voluntary exercise and environmental enrichment (EE) have been tested in EAE (Rossi et al., 2009; Benson et al., 2015; Bonfiglio et al., 2018) and both experimental settings have been found to ameliorate clinical score and, importantly, to prevent synaptic

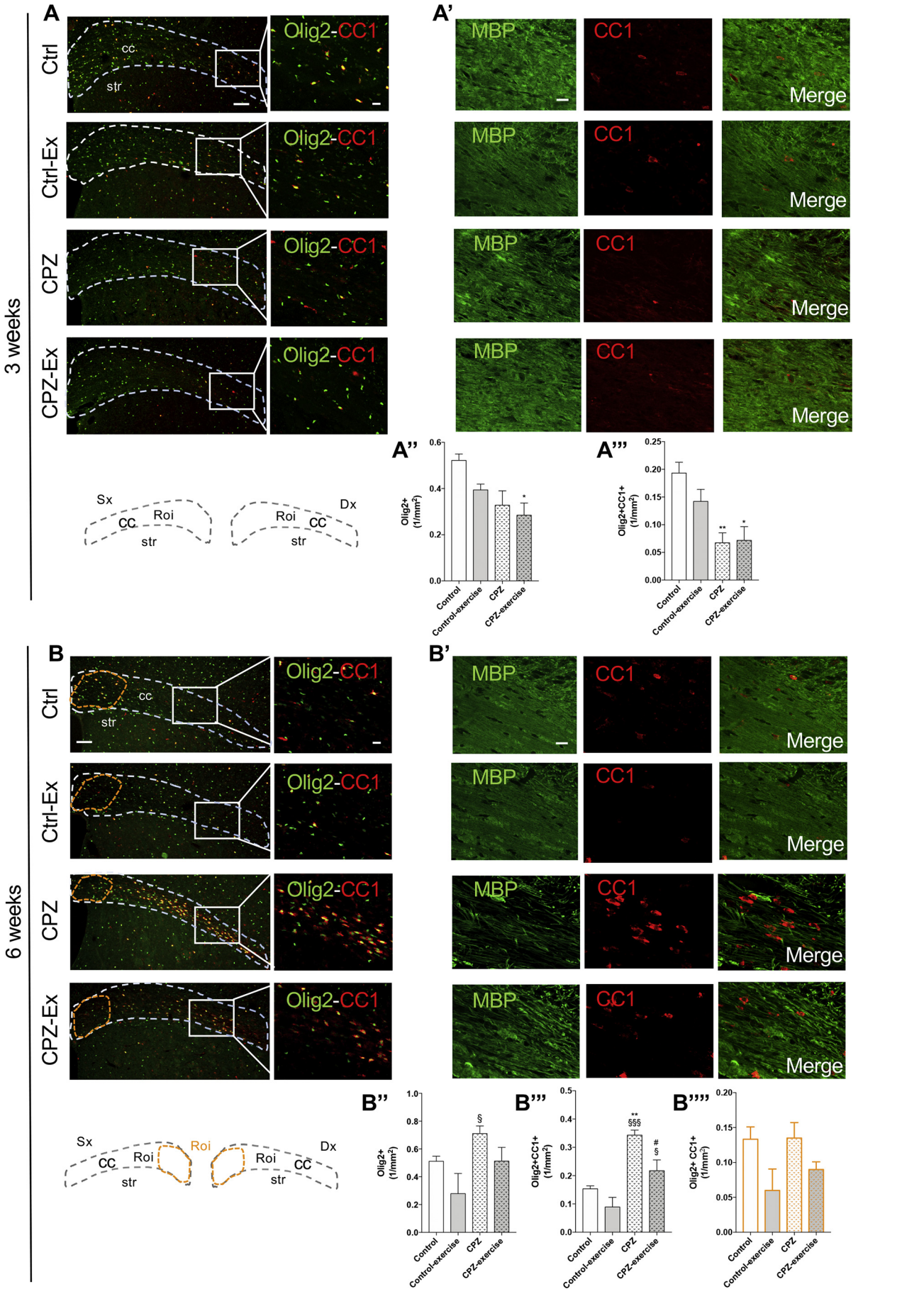

(caption on next page)

Fig. 4. Effects of exercise on Olig2+ and Olig2 + CC1+ and MBP over the course of CPZ treatment.
A-B. Representative confocal micrographs illustrating the density of cells double labelled for CC1 (red) and Olig2 cells (green) in the CC at 3 and 6 weeks of treatment. Two areas were counted, one including most of the lateral CC (white Roi area on both sides) and the other one close to the LV (orange Roi area on both sides of the CC). A. The images show the density of Olig2+ and Olig2 + CC1+ cells at 3 weeks in CC of Control, Control-exercise, CPZ, and CPZ-exercise mice (Scale bar: 100 μm). Inset on the right refers to the white boxes (Scale bar: 20 μm). A, A". The density of Olig2+ cells was reduced in CC of Control-exercise, CPZ, and CPZ-exercise mice with a significant difference between CPZ-exercise and Control mice. A, A'". The number of Olig2 + CC1+ cells was significantly reduced in both CPZ and CPZ-exercise compared to Control. B. The images show the density of Olig2+ cells at 6 weeks in CC of Control, Control-exercise, CPZ, and CPZ-exercise mice (Scale bar: 100 μm). Inset on the right refers to the white boxes (Scale bar: 20 μm). B, B″. Counting shows an increased density of Olig2+ cells in CPZ that was significantly different compared to Control-exercise group. B-B‴ At 6 weeks, CPZ induced an increase in the number of OLs (Olig2 + CC1+) that is attenuated by exercise. B-B⁗. The histogram, referred to the counting performed in the orange Roi area, highlights no significant differences among groups, but a clear trend of reduction of Olig2 + CC1+ cells induced by exercise in both Control and CPZ mice. A'-B′. In A' and B' images highlight the distribution of CC1+ cells (red) in the external part of the CC area labelled with MBP (green) at 3 (A') and 6 (B′) weeks (Scale bar: 20 μm).
One-way ANOVA, Tukey post-hoc comparisons: * $p < 0.05$, ** $p < 0.01$ *vs* Control; # $p < 0.05$ *vs* CPZ; § $p < 0.05$, §§§ $p < 0.001$ *vs* Control-exercise. (For interpretation of the references to color in this figure legend, the reader is referred to the web version of this article.)

defects in the striatum and the cortex of EAE mice (Rossi et al., 2009; Bonfiglio et al., 2018). However, the effects of such kind of natural behavioral experiences on the demyelination induced by EAE is still elusive. In CPZ mice epigenetic mechanisms involving increased expression of histone deacetylases 1/2 (HDAC1/2) have been postulated to drive the pro-remyelinating effects of environmental enrichment initiated after 6-week CPZ-intoxication (Zheng et al., 2017). It should be noted that the ability of exercise to influence myelination under physiological and pathological conditions is still poorly investigated (Tomlinson et al., 2016).

Several lines of evidence indicate that voluntary running wheel can promote myelin plasticity, by inducing the proliferation and/or differentiation of OPCs, by promoting the terminal differentiation of immature OLs into mature OLs or by improving myelination of existing OLs (Tomlinson et al., 2016). Here we found that exercise did not change MBP and CNPase levels in control mice, in line with results obtained by Tomlinson et al. (2018) in experimental conditions similar to ours (female mice, housed 2 per cage, voluntary running wheel started at age 8 weeks). Conversely, exercise partially recovered MBP and CNPase loss in white matter tracts typically affected by CPZ, such as the CC, the CG and the striatum already after 3 weeks of CPZ feeding and up to 6 weeks of treatment, suggesting that during a toxic-

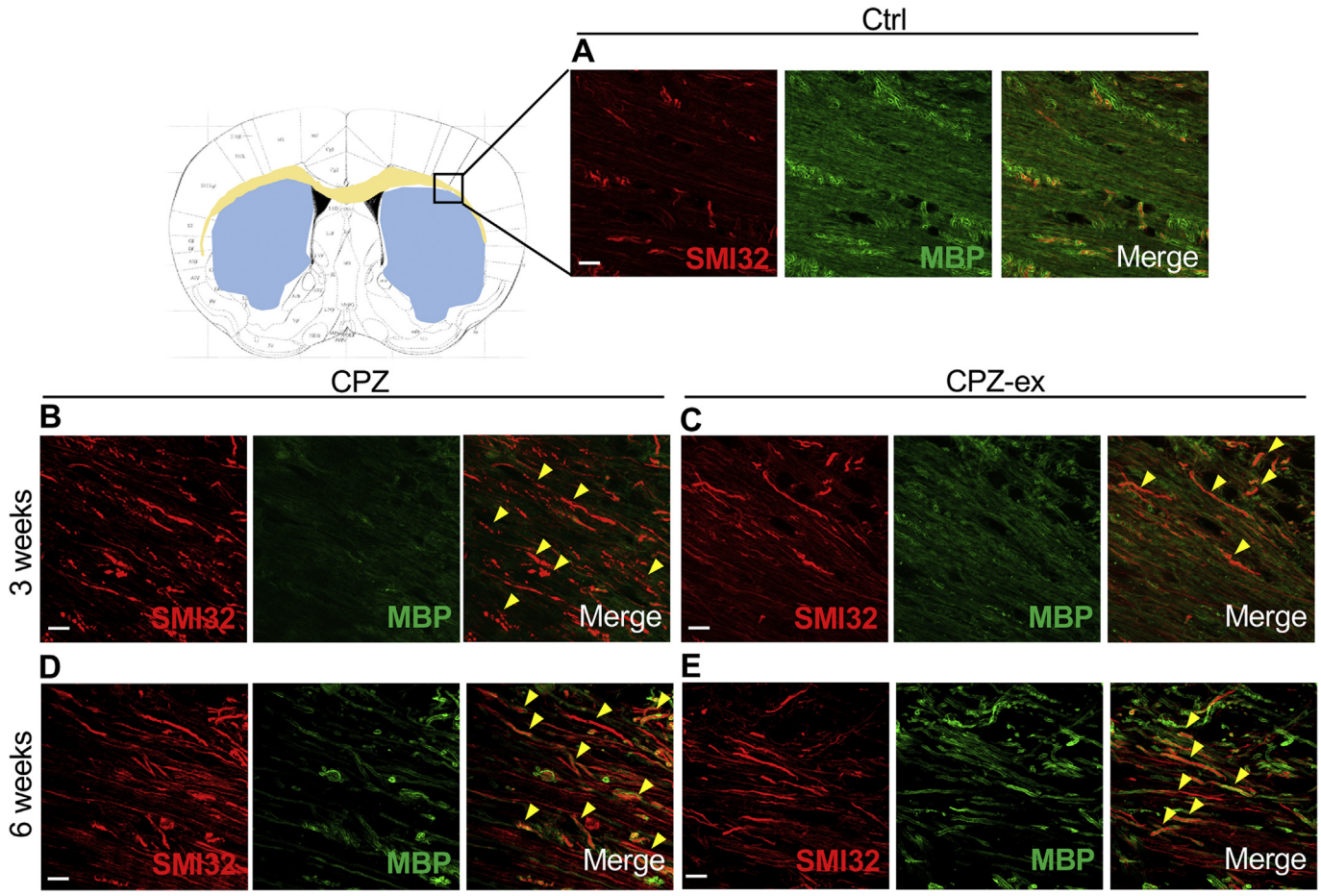

Fig. 5. Axonal pathology is ameliorated in CPZ-exercise CC.
Coronal slices from Control, CPZ and CPZ-exercise brains were stained with anti-SMI32 (red color) and MBP (green color) to assess the effect of exercise on axonal damage during the course of CPZ. In A example of SMI-32-MBP staining in the lateral callosal projections, showing the presence of few MBP + SMI32+ axons (merge). SMI32 staining is significantly increased in CPZ at both 3 (B) and 6 weeks (D). At 3 weeks in CPZ CC typical signs of axon conduction impairment are evident and highlighted by yellow arrows (B) in unmyelinated areas. In CPZ-exercise CC axonal damage is lessened at both time-point (C-E) compared to CPZ. Scale bar: 10 μm. (For interpretation of the references to color in this figure legend, the reader is referred to the web version of this article.)

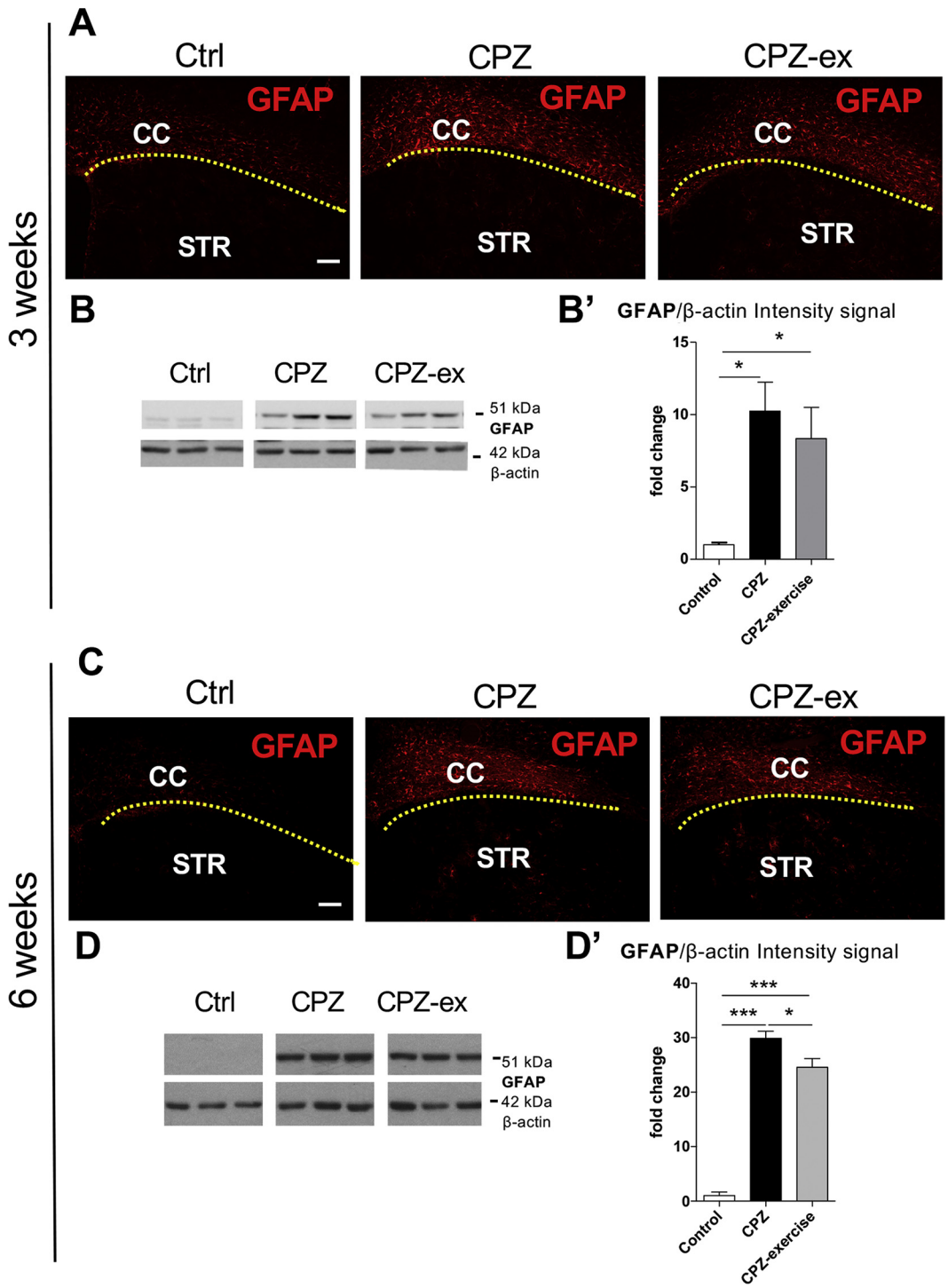

Fig. 6. Effects of exercise on astrogliosis during CPZ.
A. Immunofluorescence for GFAP marker (red color in the picture) was performed to assess astrogliosis in the CC and the striatum of mice at 3 weeks. Significant astrogliosis is observed in both areas of CPZ animals. Exercise had a slight effect on astrogliosis in both areas. Scale bar: 100 μm. B-B′ WB of total lysates were performed to assess GFAP content (≈51 kDa band on the blot, A) in Control, CPZ and CPZ-exercise groups at week 3. Densitometric analysis of the bands in B′, normalized to β-actin, reveals that CPZ treatment led to a significant increase in the level of GFAP with negligible effects of exercise. One-way ANOVA, Tukey post-hoc comparisons: ** $p < 0.05$. C. Astrogliosis was assessed by IF at 6 weeks of the experimental design. GFAP staining was slightly attenuated by exercise. Scale bar: 100 μm. D-D': WB of 6-week striatal samples confirmed IF observations. GFAP levels normalized to β-actin were significantly reduced in CPZ-exercise mice compared to CPZ. One-way ANOVA, Tukey post-hoc comparisons: ** $p < 0.05$, *** $p < 0.001$. (For interpretation of the references to color in this figure legend, the reader is referred to the web version of this article.)

demyelination insult exercise activates mechanisms/pathways aimed to increase/protect myelin content.

To this respect, at both time-points we observed an attenuated axonal pathology, which is known to occur during the course of CPZ and which is a typical hallmark of MS brains (Schultz et al., 2017). Axonal pathology, meaning the accumulation of SMI32+ axons in lateral callosal projection areas, was lessened in CPZ-exercise brains compared to CPZ, even early in the disease course and in the presence of increased

Table 2
qPCR results of striatal cytokines and chemokines at week 3 and 6 of the experimental design.

Week 3		Control n = 5	Control-Exercise n = 5	CPZ n = 5	CPZ-Exercise n = 4
Cytokines	TNF	1.02 ± 0.10	1.07 ± 0.15	8.56 ± 1.62 ***§§§	10.35 ± 0.27***§§§
	IL-1β	1.06 ± 0.17	1.28 ± 0.05	13.36 ± 0.98***§§§	12.02 ± 1.57***§§§
Chemokines	TGF-β1	1.00 ± 0.05	0.99 ± 0.06	1.64 ± 0.08***§§§	1.59 ± 0.08***§§§
	CXCL12	1.01 ± 0.07	1.06 ± 0.08	0.98 ± 0.06	0.93 ± 0.05
	CXCL10	1.01 ± 0.07	0.61 ± 0.11	21.60 ± 2.30***§§§	20.70 ± 1.58***§§§

Week 6		Control n = 3	Control-Exercise n = 3	CPZ n = 4	CPZ-Exercise n = 4
Cytokines	TNF	1.51 ± 0.82	0.30 ± 0.05	4.30 ± 0.39§§	5.18 ± 0.91*§§
	IL-1β	1.30 ± 0.67	0.78 ± 0.19	15.24 ± 3.79*§	17.82 ± 3.61*§
Chemokines	TGF-β1	1.08 ± 0.32	0.85 ± 0.06	2.42 ± 0.13**§§§	2.44 ± 0.20**§§§
	CXCL12	1.03 ± 0.17	0.95 ± 0.06	0.83 ± 0.06	0.93 ± 0.05
	CXCL10	1.12 ± 0.40	1.90 ± 0.67	32.01 ± 4.74***§§§	19.75 ± 0.47$^{**§§\#}$

Data are expressed as mean ± sem. Comparison of CPZ and CPZ-exercise to Control * $p < 0.05$, ** $p < 0.01$, *** $p < 0.001$; comparison of CPZ and CPZ-exercise to Control-exercise $^{§}p < 0.05$,§§ $p < 0.01$, §§§ $p < 0.001$; comparison between CPZ and CPZ-exercise $^{\#}p < 0.05$, $^{\#\#}p < 0.01$, $^{\#\#\#}$ $p < 0.001$. One-way ANOVA analysis, Tukey post-hoc.

myelin. Of note, disturbances in axonal conduction have been linked to the degree of disability and disease progression in MS (Singh et al., 2017). In this respect, it is worth pointing out that the data of myelin and axonal preservation were associated with functional recovery observed in CPZ mice during exercise protocol, providing evidence for the therapeutic efficacy of the voluntary exercise. Indeed, at Rotarod test motor coordination deficits typical of CPZ mice were significantly improved by exercise at the end of the experimental design. Furthermore, exercise prevented the early weight loss associated to CPZ and neuromuscular deficits in terms of fore- and hind-limbs strength by the third week of treatment.

Myelination and remyelination rely on several complex mechanisms of OPCs differentiation through different stages into mature myelinating OLs (Bercury and Macklin, 2015). We explored the possibility that exercise could protect OLs against CPZ-induced loss during the acute phase of OLs death (3 weeks) and/or promote differentiation during the spontaneous remyelinating phase of CPZ model (between 5 and 6 weeks). At 3 weeks, where there is a consistent loss of mature OLs, exercise seemed to have *per se* an effect on these cell population that lasted in chronic (6 weeks). We might suppose that exercise can favor the terminal differentiation of OLs in both healthy and pathological conditions, by down-regulating Olig2 in OLs. Indeed, it has been proposed that the downregulation of the lineage marker Olig2 induces the terminal differentiation of OLs in myelinating OLs (Mei et al., 2013). Mei and colleagues elegantly demonstrated that ablation of Olig2 in OPCs significantly reduced the number of differentiated CC1 + cells, resulting in hypomyelination, while the deletion of the Olig2 gene in immature OLs significantly enhanced the myelinating phenotype of mature OLs and resulted in improved remyelination during a 6-weeks CPZ treatment. Moreover, it has been reported that CC1 may not label the myelinating OLs (Boda et al., 2011). These data might reconcile our results of Olig2 + CC1 + counts in animals undergoing exercise with the normal myelin content observed in Control-exercise and the partially preserved myelin of CPZ-exercise, respectively. This suggests that during the phase of maximal OLs loss caused by CPZ (3 weeks), exercise may preserve or enhance the density of fully myelinating OLs. This hypothesis might apply also to results obtained at 6 weeks, where a reduced recruitment of new OLs was observed in CPZ-exercise compared to CPZ mice. Another possibility is that the early preservation of myelin exerted by exercise might recruit less OLs during the sixth week of CPZ treatment. Indeed, at this time-point we highlighted an overproduction of new OLs in CPZ CC and particularly evident in the lateral CC, that is highly sensitive to CPZ-induced damage (Pott et al., 2009, present study). During the phase of spontaneous remyelination, the strong damage caused by CPZ in this area may promote a more efficient recruitment of OPCs that, however, turns into an unsuccessful myelination. In contrast, in CPZ-exercise the density of new OLs was similar to control and significantly lower compared to CPZ, in the presence of increased myelin density, likely as the consequence of the early prevention of myelin loss induced by exercise.

Another important finding of our study is that exercise attenuated astrogliosis and to a much larger extent microgliosis in both the CC and the striatum. In CNS, activation of microglia and astrocytosis are important components of the lesion environment that can impact demyelination process, and these cells have been crucially involved in demyelination/remyelination processes during CPZ (Gudi et al., 2014). The role of astrocytes in the CPZ model is still not completely elucidated. It has been demonstrated that activation of astrocytic NF-κB can lead to oligodendrocyte damage; on the contrary, attenuation of NF-κB signaling has been found protective against myelin loss, pro-inflammatory response, and reactive gliosis (Raasch et al., 2011; Brück et al., 2012). Experiments of selective glial ablation in CPZ mice have clearly demonstrated that astrocytes recruit microglia *via* CXCL10 to perform myelin debris removal, suggesting that microglia can promote remyelination (Skripuletz et al., 2013). In contrast, it has been suggested that microglia, recruited by soluble mediators released by astrocytes, actively participates to demyelinating events (Plant et al., 2005). In our study we observed a minor effect of exercise on astrogliosis, which was significant only at week 6 of CPZ treatment in coincidence of a reduction of CXCL10 (qPCR). Moreover, we could not detect significant differences in terms of cytokines and chemokines in striatal lysates of CPZ and CPZ-exercise, suggesting that, at least limited to the analyzed molecules, the inflammatory milieu was not affected by exercise. However, the striking effect of exercise on microglia observed already at 3 weeks underlies the possibility that exercise acts on microglia independently of the astroglia-microglia axis, in particular at week 3. Moreover, we cannot rule out that exercise creates a less toxic environment even before the point of maximal accumulation of microglia corresponding to 3–4 weeks of CPZ intoxication, leading to the reduced recruitment of microglia already at this time-point. This hypothesis is supported by the finding that in CPZ-exercise myelin content is preserved even at 3 weeks, suggesting a protective role of exercise. Together with data from myelin studies, we suggest that the reduced myelin damage promoted by exercise might limit the recruitment of microglia in the damaged white matter area. This, in turn, might lay the ground for the less recruitment of new OLs during the late phase of CPZ feeding.

7. Conclusions

In conclusion, our study demonstrates that voluntary exercise has an impact on the main pathological hallmarks of CPZ mice and likely in

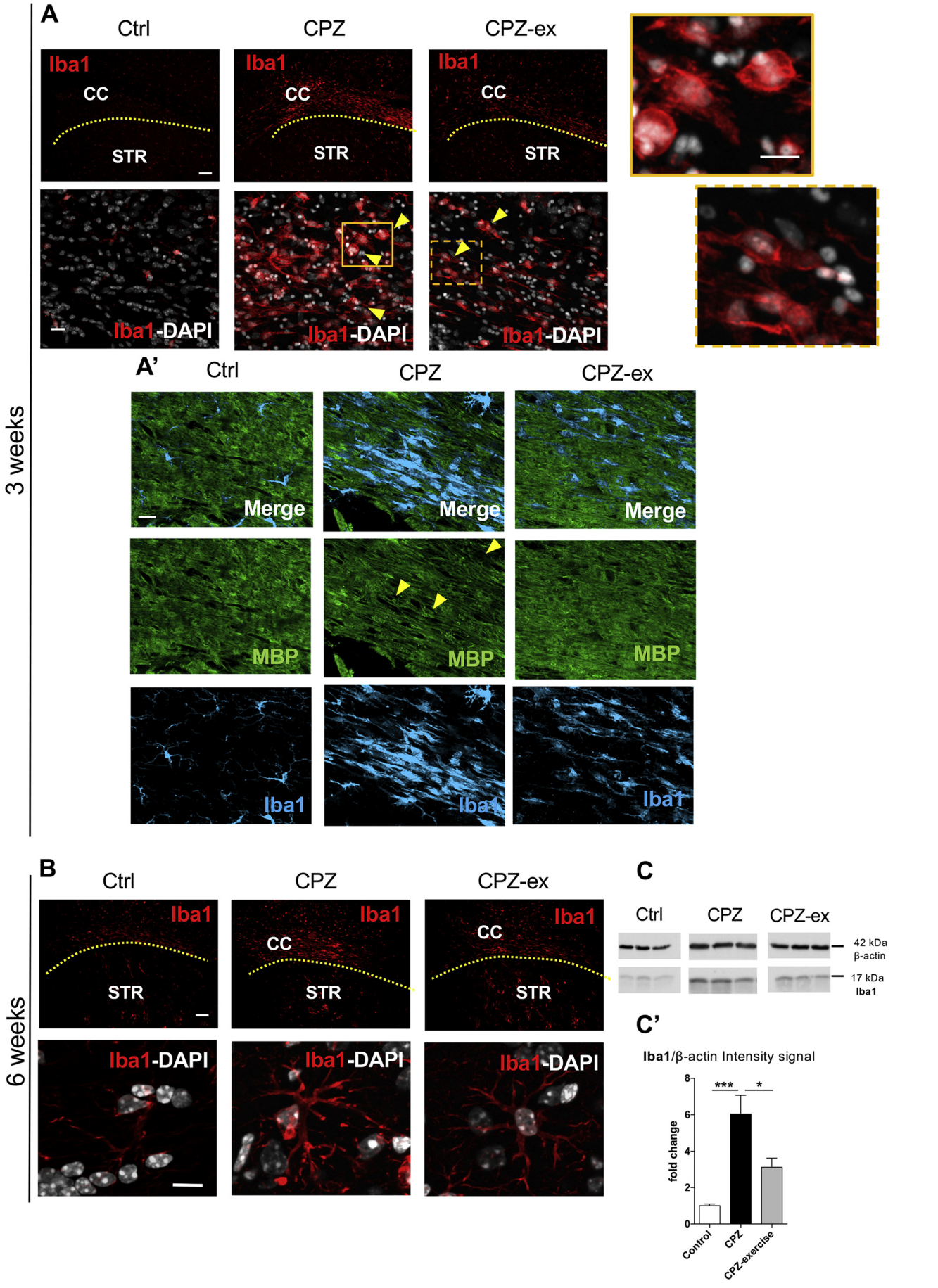

(caption on next page)

Fig. 7. Microgliosis is significantly attenuated in running wheel CPZ mice.
Microgliosis in the CC and the striatum was assessed by IF. A. At 3 weeks Iba1 staining (in red) was significantly increased in the CC and the striatum of CPZ mice and exercise induced a striking reduction of microglia proliferation (scale bar: 100 μm). Lower panel shows the morphology of Iba1 + cells with ameboid Iba1 + cells more frequently detected in CPZ than CPZ-exercise (yellow arrows). Nuclei were stained with DAPI (in grey; scale bar: 20 μm). Inset on the right refers to the orange box in CPZ and CPZ-exercise panel (scale bar: 20 μm). A'. Confocal images highlight the loss of MBP staining (green, yellow arrows) in striatal slices in the presence of increase of microglia infiltrates in CPZ CC. Microgliosis was reduced in CPZ-exercise and MBP staining was more similar to Control slice. Scale bar: 20 μm. B. The effect of exercise on microgliosis lasted to the sixth week of CPZ treatment as shown in low magnification pictures (scale bar: 100 μm). High magnification images, on the bottom, highlight differences in the morphology of the Iba1 + cells (counterstained with DAPI) among Control (resting microglia), CPZ (activated microglia) and CPZ-exercise (intermediate phenotype; scale bar: 10 μm). C. WB was performed to analyze the levels of Iba1 in striatal lysates of Control, CPZ and CPZ-exercise mice. C′. Quantitative analysis of Iba1 signal normalized to β-actin shows that exercise significantly reduced the CPZ-induced Iba1 upregulation. One-way ANOVA, Tukey post-hoc comparisons: * $p < 0.05$;*** $p < 0.001$. (For interpretation of the references to color in this figure legend, the reader is referred to the web version of this article.)

MS, namely demyelination, axonal pathology, microgliosis and astrogliosis, independently of the peripheral immunomodulation. By translating our results to human pathology and management, our data suggest that promoting MS patient engagement in physical activity tightly tailored to their degree of disability represent a good non-pharmacological tool to control disease progression.

Acknowledgement

The authors thank Massimo Tolu for helpful technical assistance, Dr. Francesca De Santa from Institute of Cell Biology and Neurobiology (IBCN), National Research Council of Italy (CNR), Rome and Dr. Giacomo Paonessa, Head of Molecular Biology at IRBM Science Park, Pomezia) for their support in qPCR experiments.

Funding and disclosure

This work was supported by the Italian Ministry of Health (Ricerca corrente—IRCCS San Raffaele Pisana; Ricerca corrente—IRCCS Neuromed and 5 × 1000-IRCCS Neuromed) and by FISM -Fondazione Italiana Sclerosi Multipla- cod. 2019/S/1 to DC and FRR and financed or co-financed with the “5 per mille” public funding. AG was supported by Fondazione Veronesi fellowship. The authors declare no competing financial interests.

References

Andreasen, A., Stenager, E., Dalgas, U., 2011. The effect of exercise therapy on fatigue in multiple sclerosis. Mult. Scler. J. 17 (9), 1041–1054. https://doi.org/10.1177/1352458511401120.

Barry, A., Cronin, O., Ryan, A.M., Sweeney, B., Yap, S.M., O'Toole, O., Allen, A.P., Clarke, G., O'Halloran, K.D., Downer, E.J., 2016. Impact of exercise on innate immunity in multiple sclerosis progression and symptomatology. Front. Physiol. 7, 194. https://doi.org/10.3389/fphys.2016.00194.

Baxi, E.G., DeBruin, J., Jin, J., Strasburger, H.J., Smith, M.D., Orthmann-Murphy, J.L., Schott, J.T., Fairchild, A.N., Bergles, D.E., Calabresi, P.A., 2017. Lineage tracing reveals dynamic changes in oligodendrocyte precursor cells following cuprizone-induced demyelination. Glia 65 (12), 2087–2098. https://doi.org/10.1002/glia.23229. (Epub 2017 Sep 22).

Benson, C., Paylor, J.W., Tenorio, G., Winship, I., Baker, G., Kerr, B.J., 2015. Voluntary wheel running delays disease onset and reduces pain hypersensitivity in early experimental autoimmune encephalomyelitis (EAE). Exp. Neurol. 271, 279–290. https://doi.org/10.1016/j.expneurol.2015.05.017.

Bercury, K.K., Macklin, W.B., 2015. Dynamics and mechanisms of CNS myelination. Dev. Cell 32 (4), 447–458. https://doi.org/10.1016/j.devcel.2015.01.016.

Boda, E., Viganò, F., Rosa, P., Fumagalli, M., Labat-Gest, V., Tempia, F., Abbracchio, M.P., Dimou, L., Buffo, A., 2011. The GPR17 receptor in NG2 expressing cells: focus on in vivo cell maturation and participation in acute trauma and chronic damage. Glia 59, 1958–1973.

Bonfiglio, T., Olivero, G., Vergassola, M., Di Cesare Mannelli, L., Pacini, A., Iannuzzi, F., Summa, M., Bertorelli, R., Feligioni, M., Ghelardini, C., Pittaluga, A., 2018. Environmental training is beneficial to clinical symptoms and cortical presynaptic defects in mice suffering from experimental autoimmune encephalomyelitis. Neuropharmacology. https://doi.org/10.1016/j.neuropharm.2018.01.026. pii: S0028-3908(18)30026-1.

Brück, W., Pförtner, R., Pham, T., Zhang, J., Hayardeny, L., Piryatinsky, V., Hanisch, U.K., Regen, T., van Rossum, D., Brakelmann, L., Hagemeier, K., Kuhlmann, T., Stadelmann, C., John, G.R., Kramann, N., Wegner, C., 2012. Reduced astrocytic NF-κB activation by laquinimod protects from cuprizone-induced demyelination. Acta Neuropathol. 124 (3), 411–424. https://doi.org/10.1007/s00401-012-1009-1.

Buschmann, J.P., Berger, K., Awad, H., Clarner, T., Beyer, C., Kipp, M., 2012. Inflammatory response and chemokine expression in the white matter corpus callosum and gray matter cortex region during cuprizone-induced demyelination. J. Mol. Neurosci. 48 (1), 66–76. https://doi.org/10.1007/s12031-012-9773-x.

Clarner, T., Diederichs, F., Berger, K., Denecke, B., Gan, L., van der Valk, P., Beyer, C., Amor, S., Kipp, M., 2012. Myelin debris regulates inflammatory responses in an experimental demyelination animal model and multiple sclerosis lesions. Glia 60 (10), 1468–1480. https://doi.org/10.1002/glia.22367.

Cotman, C.W., Berchtold, N.C., 2002. Exercise: a behavioral intervention to enhance brain health and plasticity. Trends Neurosci. 25 (6), 295–301 2002 Jun.

Dalgas, U., Stenager, E., Ingemann-Hansen, T., 2008. Multiple sclerosis and physical exercise: recommendations for the application of resistance-, endurance- and combined training. Mult. Scler. 14 (1), 35–53. https://doi.org/10.1177/1352458507079445.

Dalgas, U., Stenager, E., Jakobsen, J., Petersen, T., Hansen, H.J., Knudsen, C., Overgaard, K., Ingemann-Hansen, T., 2009. Resistance training improves muscle strength and functional capacity in multiple sclerosis. Neurology 73 (18), 1478–1484. https://doi.org/10.1212/WNL.0b013e3181bf98b4.

Domingues, H.S., Portugal, C.C., Socodato, R., Relvas, J.B., 2016. Oligodendrocyte, astrocyte, and microglia crosstalk in myelin development, damage, and repair. Front. Cell. Dev. Biol. 4, 71. https://doi.org/10.3389/fcell.2016.00071. (eCollection 2016. Review. Erratum in: Front. Cell. Dev. Biol. 2016 4:79).

Ensari, I., Motl, R.W., Pilutti, L.A., 2014. Exercise training improves depressive symptoms in people with multiple sclerosis: results of a meta-analysis. J. Psychosom. Res. 76 (6), 465–471. https://doi.org/10.1016/j.jpsychores.2014.03.014.

Gentile, A., Fresegna, D., Federici, M., Musella, A., Rizzo, F.R., Sepman, H., Bullitta, S., De Vito, F., Haji, N., Rossi, S., Mercuri, N.B., Usiello, A., Mandolesi, G., Centonze, D., 2015. Dopaminergic dysfunction is associated with IL-1β-dependent mood alterations in experimental autoimmune encephalomyelitis. Neurobiol. Dis. 74, 347–358. https://doi.org/10.1016/j.nbd.2014.11.022.

Goh, J., Ladiges, W., 2015. Voluntary wheel running in mice. Curr. Protoc. Mouse Biol. 5 (4), 283–290. https://doi.org/10.1002/9780470942390.mo140295.

Grace, A.A., 2002. Dopamine. In: Davis, K.L., Charney, D.S., Coyle, J.T., Nemeroff, C.B. (Eds.), Neuropsychopharmacology: The Fifth Generation of Progress. Lippincott Williams and Wilkins, Philadelphia, pp. 119–132.

Gudi, V., Gingele, S., Skripuletz, T., Stangel, M., 2014. Glial response during cuprizone-induced de- and remyelination in the CNS: lessons learned. Front. Cell. Neurosci. 8, 73. https://doi.org/10.3389/fncel.2014.00073.

Gudi, V., Gai, L., Herder, V., Tejedor, L.S., Kipp, M., Amor, S., Sühs, K.W., Hansmann, F., Beineke, A., Baumgärtner, W., Stangel, M., Skripuletz, T., 2017. Synaptophysin is a reliable marker for axonal damage. J. Neuropathol. Exp. Neurol. https://doi.org/10.1093/jnen/nlw114.

Hashimoto, M., Yamamoto, S., Iwasa, K., Yamashina, K., Ishikawa, M., Maruyama, K., Bosetti, F., Yoshikawa, K., 2017. The flavonoid Baicalein attenuates cuprizone-induced demyelination via suppression of neuroinflammation. Brain Res. Bull. 135, 47–52. https://doi.org/10.1016/j.brainresbull.2017.09.007.

Herbst, E.A., Holloway, G.P., 2015. Exercise training normalizes mitochondrial respiratory capacity within the striatum of the R6/1 model of Huntington's disease. Neuroscience 303, 515–523. https://doi.org/10.1016/j.neuroscience.2015.07.025.

Hiremath, M.M., Saito, Y., Knapp, G.W., Ting, J.P., Suzuki, K., Matsushima, G.K., 1998. Microglial/macrophage accumulation during cuprizone-induced demyelination in C57BL/6 mice. J. Neuroimmunol. 92 (1–2), 38–49.

Kipp, M., Clarner, T., Dang, J., Copray, S., Beyer, C., 2009. The cuprizone animal model: new insights into an old story. Acta Neuropathol. 118 (6), 723–736. https://doi.org/10.1007/s00401-009-0591-3.

Klein, C., Rasińska, J., Empl, L., Sparenberg, M., Poshtiban, A., Hain, E.G., Iggena, D., Rivalan, M., Winter, Y., Steiner, B., 2016. Physical exercise counteracts MPTP-induced changes in neural precursor cell proliferation in the hippocampus and restores spatial learning but not memory performance in the water maze. Behav. Brain Res. 307, 227–238. https://doi.org/10.1016/j.bbr.2016.02.040.

Kondo, M.A., Gray, L.J., Pelka, G.J., Leang, S.K., Christodoulou, J., Tam, P.P., Hannan, A.J., 2016. Affective dysfunction in a mouse model of Rett syndrome: therapeutic effects of environmental stimulation and physical activity. Dev. Neurobiol. 76 (2), 209–224. https://doi.org/10.1002/dneu.22308.

Kutzelnigg, A., Lassmann, H., 2014. Pathology of multiple sclerosis and related inflammatory demyelinating diseases. Handb. Clin. Neurol. 122, 15–58. https://doi.org/10.1016/B978-0-444-52001-2.00002-9.

Lublin, F.D., 2005. Clinical features and diagnosis of multiple sclerosis. Neurol. Clin. 23, 1–15. https://doi.org/10.1016/j.ncl.2004.09.003.

Lucchinetti, C., Brück, W., Parisi, J., Scheithauer, B., Rodriguez, M., Lassmann, H., 2000.

Heterogeneity of multiple sclerosis lesions: implications for the pathogenesis of demyelination. Ann. Neurol. 47 (6), 707–717.
Lynch, M.A., 2009. The multifaceted profile of activated microglia. Mol. Neurobiol. 40 (2), 139–156. https://doi.org/10.1007/s12035-009-8077-9.
Mason, J.L., Jones, J.J., Taniike, M., Morell, P., Suzuki, K., Matsushima, G.K., 2000. Mature oligodendrocyte apoptosis precedes IGF-1 production and oligodendrocyte progenitor accumulation and differentiation during demyelination/remyelination. J. Neurosci. Res. 61 (3), 251–262. https://doi.org/10.1002/1097-4547(20000801)61:3<251::AID-JNR3>3.0.CO;2-W.
Matsushima, G.K., Morell, P., 2001. The neurotoxicant, cuprizone, as a model to study demyelination and remyelination in the central nervous system. Brain Pathol. 11 (1), 107–116.
Mei, F., Wang, H., Liu, S., Niu, J., Wang, L., He, Y., Etxeberria, A., Chan, J.R., Xiao, L., 2013. Stage-specific deletion of Olig2 conveys opposing functions on differentiation and maturation of oligodendrocytes. J. Neurosci. 33 (19), 8454–8462. https://doi.org/10.1523/JNEUROSCI.2453-12.2013.
Morell, P., Barrett, C.V., Mason, J.L., Toews, A.D., Hostettler, J.D., Knapp, G.W., Matsushima, G.K., 1998. Gene expression in brain during cuprizone-induced demyelination and remyelination. Mol. Cell. Neurosci. 12 (4–5), 220–227. https://doi.org/10.1006/mcne.1998.0715.
Motl, R.W., Pilutti, L.A., 2012. The benefits of exercise training in multiple sclerosis. Nat. Rev. Neurol. 8, 487–497. https://doi.org/10.1038/nrneurol.2012.136.
Muraro, P.A., Kalbus, M., Afshar, G., McFarland, H.F., Martin, R., 2002. T cell response to 2′,3′-cyclic nucleotide 3′-phosphodiesterase (CNPase) in multiple sclerosis patients. J. Neuroimmunol. 130 (1–2), 233–242.
Patten, A.R., Sickmann, H., Hryciw, B.N., Kucharsky, T., Parton, R., Kernick, A., Christie, B.R., 2013. Long-term exercise is needed to enhance synaptic plasticity in the hippocampus. Learn. Mem. 20 (11), 642–647. https://doi.org/10.1101/lm.030635.113.
Pilutti, L.A., Greenlee, T.A., Motl, R.W., Nickrent, M.S., Petruzzello, S.J., 2013. Effects of exercise training on fatigue in multiple sclerosis: a meta-analysis. Psychosom. Med. 75 (6), 575–580. https://doi.org/10.1097/PSY.0b013e31829b4525.
Pilutti, L.A., Platta, M.E., Motl, R.W., Latimer-Cheung, A.E., 2014. The safety of exercise training in multiple sclerosis: a systematic review. J. Neurol. Sci. 343, 3–7. https://doi.org/10.1016/j.jns.2014.05.016.
Plant, S.R., Arnett, H.A., Ting, J.P., 2005. Astroglial-derived lymphotoxin-alpha exacerbates inflammation and demyelination, but not remyelination. Glia 49 (1), 1–14. https://doi.org/10.1002/glia.20089.
Popescu, B.F., Lucchinetti, C.F., 2012. Pathology of demyelinating diseases. Annu. Rev. Pathol. 7, 185–217. https://doi.org/10.1146/annurev-pathol-011811-132443.
Pott, F., Gingele, S., Clarner, T., Dang, J., Baumgartner, W., Beyer, C., Kipp, M., 2009. Cuprizone effect on myelination, astrogliosis and microglia attraction in the mouse basal ganglia. Brain Res. 1305, 137–149. https://doi.org/10.1016/j.brainres.2009.09.084.
Praet, J., Guglielmetti, C., Berneman, Z., Van der Linden, A., Ponsaerts, P., 2014. Cellular and molecular neuropathology of the cuprizone mouse model: clinical relevance for multiple sclerosis. Neurosci. Biobehav. Rev. 47, 485–505. https://doi.org/10.1016/j.neubiorev.2014.10.004.
Raasch, J., Zeller, N., van Loo, G., Merkler, D., Mildner, A., Erny, D., Knobeloch, K.P., Bethea, J.R., Waisman, A., Knust, M., Del Turco, D., Deller, T., Blank, T., Priller, J., Brück, W., Pasparakis, M., Prinz, M., 2011. IkappaB kinase 2 determines oligodendrocyte loss by non-cell-autonomous activation of NF-kappaB in the central nervous system. Brain 134 (Pt4), 1184–1198. https://doi.org/10.1093/brain/awq359.
Rossi, S., Furlan, R., De Chiara, V., Musella, A., Lo Giudice, T., Mataluni, G., Cavasinni, F., Cantarella, C., Bernardi, G., Muzio, L., Martorana, A., Martino, G., Centonze, D., 2009. Exercise attenuates the clinical, synaptic and dendritic abnormalities of experimental autoimmune encephalomyelitis. 36 (1), 51–59. https://doi.org/10.1016/j.nbd.2009.06.013.
Schultz, V., van der Meer, F., Wrzos, C., Scheidt, U., Bahn, E., Stadelmann, C., Brück, W., Junker, A., 2017. Acutely damaged axons are remyelinated in multiple sclerosis and experimental models of demyelination. Glia 65 (8), 1350–1360. https://doi.org/10.1002/glia.23167.
Singh, S., Dallenga, T., Winkler, A., Roemer, S., Maruschak, B., Siebert, H., Brück, W., Stadelmann, C., 2017. Relationship of acute axonal damage, Wallerian degeneration, and clinical disability in multiple sclerosis. J. Neuroinflammation 14 (1), 57. https://doi.org/10.1186/s12974-017-0831-8.
Skripuletz, T., Hackstette, D., Bauer, K., Gudi, V., Pul, R., Voss, E., Berger, K., Kipp, M., Baumgärtner, W., Stangel, M., 2013. Astrocytes regulate myelin clearance through recruitment of microglia during cuprizone-induced demyelination. Brain 136 (Pt1), 147–167. https://doi.org/10.1093/brain/aws262.
Stidworthy, M.F., Genoud, S., Suter, U., Mantei, N., Franklin, R.J., 2003. Quantifying the early stages of remyelination following cuprizone-induced demyelination. Brain Pathol. 13 (3), 329–339.
Tapia-Rojas, C., Aranguiz, F., Varela-Nallar, L., Inestrosa, N.C., 2016. Voluntary running attenuates memory loss, decreases Neuropathological changes and induces neurogenesis in a mouse model of Alzheimer's disease. Brain Pathol. 26 (1), 62–74. https://doi.org/10.1111/bpa.12255.
Tomlinson, L., Leiton, C.V., Colognato, H., 2016. Behavioral experiences as drivers of oligodendrocyte lineage dynamics and myelin plasticity. Neuropharmacology 110 (Pt B), 548–562. https://doi.org/10.1016/j.neuropharm.2015.09.016.
Tomlinson, L., Huang, P.H., Colognato, H., 2018. Prefrontal cortex NG2 undergo a developmental switch in their responsiveness to exercise. Dev Neurobiol 78 (7), 687–700. https://doi.org/10.1002/dneu.22590.
Trapp, B.D., Peterson, J., Ransohoff, R.M., Rudick, R., Mörk, S., Bö, L., 1998. Axonal transection in the lesions of multiple sclerosis. N. Engl. J. Med. 338 (5), 278–285.
van den Berg, M., Dawes, H., Wade, D.T., Newman, M., Burridge, J., Izadi, H., Sackley, C.M., 2006. Treadmill training for individuals with multiple sclerosis: a pilot randomised trial. J. Neurol. Neurosurg. Psychiatry 77, 531–533. https://doi.org/10.1136/jnnp.2005.064410.
van Praag, H., Kempermann, G., Gage, F.H., 2000. Neural consequences of environmental enrichment. Nat. Rev. Neurosci. 1 (3), 191–198. https://doi.org/10.1038/35044558.
Ye, J.N., Chen, X.S., Su, L., Liu, Y.L., Cai, Q.Y., Zhan, X.L., Xu, Y., Zhao, S.F., Yao, Z.X., 2013. Progesterone alleviates neural behavioral deficits and demyelination with reduced degeneration of oligodendroglial cells in cuprizone-induced mice. PLoS ONE 8 (1), e54590. https://doi.org/10.1371/journal.pone.0054590.
Yoon, H., Kleven, A., Paulsen, A., Kleppe, L., Wu, J., Ying, Z., Gomez-Pinilla, F., Scarisbrick, I.A., 2016. Interplay between exercise and dietary fat modulates myelinogenesis in the central nervous system. Biochim. Biophys. Acta 1862 (4), 545–555. https://doi.org/10.1016/j.bbadis.2016.01.019.
Yuan, A., Rao, M.V., Veeranna, Nixon, R.A., 2017. Neurofilaments and Neurofilament proteins in health and disease. Cold Spring Harb. Perspect. Biol. 9 (4). https://doi.org/10.1101/cshperspect.a018309. pii: a018309.
Zheng, J., Ding, W., Li, B., Yang, Y., 2017. Enriched environment promotes remyelination and motor function recovery through modulation of HDAC1/2 in mice. Neurosci. Lett. 655, 121–130. https://doi.org/10.1016/j.neulet.2017.06.039.
Zipp, F., Aktas, O., 2006. The brain as a target of inflammation: common pathways link inflammatory and neurodegenerative diseases. Trends Neurosci. 29, 518–527. https://doi.org/10.1016/j.tins.2006.07.006.